

**REAL-TIME DECODING OF ARM KINEMATICS
DURING GRASPING BASED ON F5
NEURAL SPIKE DATA**

A Thesis

by

Narges Ashena

Submitted to the
Graduate School of Sciences and Engineering
In Partial Fulfillment of the Requirements for
the Degree of

Master of Science

in the
Department of Computer Science

Özyeğin University
May 2017

Copyright © 2017 by Narges Ashena

**REAL-TIME DECODING OF ARM KINEMATICS
DURING GRASPING BASED ON F5
NEURAL SPIKE DATA**

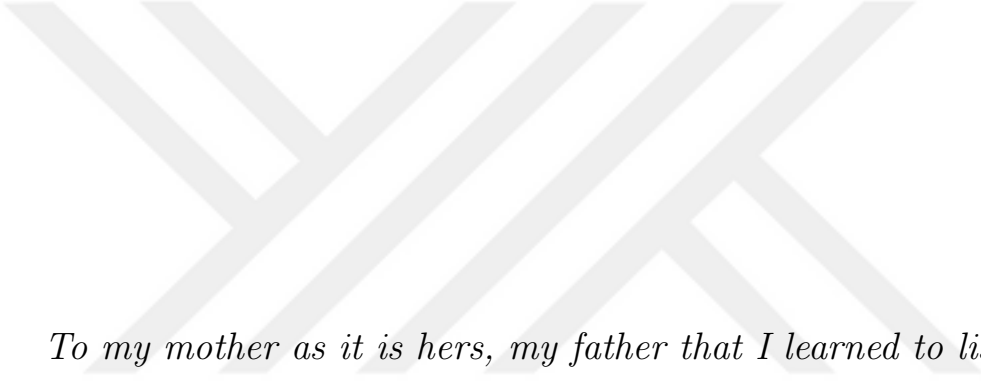
Approved by:

Associate Professor Erhan Öztop, Advisor
Department of Computer Science
Özyeğin University

Assistant Professor Emre Uğur
Department of Computer Engineering
Boğaziçi University

Assistant Professor Emrah Aktunç
Department of Psychology
Özyeğin University

Date Approved: 25th May 2017



*To my mother as it is hers, my father that I learned to listen to his
silence, and Sina for his unconditional support*

ABSTRACT

Extending our knowledge about brain mechanisms and behavior can lead to many advantages from shedding light on the diagnosis of nervous system diseases and injuries to inspiring the current state of the art in robotics and artificial intelligence.

Ventral premotor cortex, i.e. area F5, in a macaque monkey's brain is one of the areas of interest in the literature. Studies have shown that F5 area in monkeys is involved in arm movements and hand configuration, enabling the animal to grasp objects with different shapes (different grip types). Furthermore, it is shown in the studies that F5 area contains neurons called mirror neurons which are active not only during the period the animal moves his arm and hand but also while the animal is observing another monkey or person performing the same action.

In this study, we aim to investigate whether, by using F5 area neural activity, monkey's arm kinematics can be decoded in real-time or not. Furthermore, how the decoding capacity of mirror and non-mirror neurons can be differentiated. To this end, the neural behavior of 32 neurons (including mirror and non-mirror neurons) in the stated area was recorded while a monkey was performing grasping tasks on different objects. Also, monkey's motion was video captured simultaneously. Using image processing techniques and tools, kinematics data was extracted from the videos. Later, the possibility of single neuron's decoding of the kinematics data was investigated.

Results reveal that although single neuron real-time decoding of the kinematics is not always ideal, reasonable performance is achievable with selected neurons from both groups. Based on the results of this study non-mirror neurons seem to act as

better single-neuron decoders. Although it seems obvious that population-level activity is required for more robust decoding, neurons in the F5 area can be categorized based on their success measure in single-neuron decoding.



ÖZETÇE

Beyin mekanizmaları ve davranışıyla ilgili bilgimizi genişletmek, sinir sistemi hastalıklarının ve yaralanmaların teşhisine ışık tutmaktan mevcut olan en gelişkin robotik ve yapay zekâ alanlarına ilham vermeye kadar pek çok avantaj sağlayabilir.

Makaklardaki ventral premotor korteks, yani F5 bölgesi, literatürdeki ilgi alanlarından biridir. Araştırmalar, maymunlardaki F5 alanının kol hareketleri ve el konfigürasyonunda rol oynadığı ve farklı şekillerdeki objelerin (farklı kavrama tipleri) kavranmasını sağladığını gösteriyor. Ayrıca f5 alanında sadece hayvanın hareketi sırasında değil, başka bir maymunun aynı hareketini izlerken de aktif olan ayna-nöron adı verilen nöronların bulunduğu gösterilmiştir.

Bu çalışmada, F5 alanındaki sinir aktivitesini kullanarak maymunun kol kinematığının gerçek zamanlı olarak çözülüp çözilemeyeceğini, dahası, ayna ve ayna olmayan nöronların şifre çözme kapasitesinin nasıl ayırt edilebileceğini araştırmayı amaçlıyoruz. Bu amaçla, belirtilen bölgedeki 32 nöronun (ayna ve ayna olmayan nöronlar dahil) sinirsel davranışları, bir maymun farklı nesnelere üzerinde kavrama görevleri yürütürken kaydedilmiştir. Ayrıca, maymunun hareketi aynı anda videoya çekilmiştir. Görüntü işleme teknikleri ve araçlarını kullanarak videolardan kinematik veriler çıkarılmıştır. Daha sonra, tek bir nöronun kinematik verileri çözme yeteneği araştırılmıştır.

Sonuçlar, kinematiklerin tek bir nöron tarafından gerçek zamanlı kod çözümü her zaman ideal olmasa da, her iki gruptan seçilen nöronlarla makul bir performansa ulaşabileceğini ortaya koymaktadır. Bu çalışmanın sonuçlarına dayanarak, ayna olmayan nöronların tek nöronlu kod çözümleri olarak daha iyi oldukları söylenebilir. Daha güçlü kod çözme için çoklu nöron etkinliğine ihtiyaç duyulduğu açıkça görülse

de, F5 bölgesindeki nöronlar, tek nöron şifre çözme yöntemindeki başarı ölçülerine göre kategorize edilebilir.



ACKNOWLEDGEMENTS

I will take this opportunity to thank my adviser Dr. Erhan Öztop for giving me the chance of being his Master student. His patient, considerate and kind supervision paved the way for me through the academic and research life. This experience helped me change the direction of my life to the path I have always wished.

I would also like to thank Dr. Emre Uğur and Dr. Emrah Aktunç, members of thesis defense committee, for their precious feedbacks and sharing their knowledge which helped me improve my thesis.

I extend my thanks to our research collaborators from the University of Crete, Vassilis Raos and Vassilis Papadourakis, for providing us the data and sharing their valuable opinions about the analysis.

My thanks also go to the other directors of Özyeğin Robotics Lab, Dr. Ozkan Bebek and Dr. Barkan Uğurlu, for providing us scientific but friendly environment in the lab.

I owe a lot of thanks to my friends in Özyeğin. They made my time enjoyable by their friendship during my study in Özyeğin. Specifically, I am very thankful to two of my colleagues Awais Mirza Ahmad and Osman Kaya for helping me and encouraging me whenever I needed.

I would also like to thank my friends outside the university, Nassim Brojian, Lale Attar, and Aysan Nemati, for their undeniable impact on my life.

Special thanks to my dear husband, Sina, for providing me unconditional support all the time. I will be always thankful to my parents for their endless encouragement and my brothers for giving me the bravery to stand against any gender discrimination. And last but not least, I am so grateful to my husband family for giving the

priority to my study all the times. This research was supported by the grant OBSER-
VENEMO within the framework of the bilateral S&T Cooperation Program between
the Republic of Turkey and the Hellenic Republic. Grant No. 113S391 funded by
TUBITAK and grant ITET 14UR OBSERVENEMO co-Financed by the European
Union and the Greek State, MCERA/GSRT.



TABLE OF CONTENTS

DEDICATION	iii
ABSTRACT	iv
ÖZETÇE	vi
ACKNOWLEDGEMENTS	viii
LIST OF TABLES	xii
LIST OF FIGURES	xiii
I INTRODUCTION	1
1.1 Related Works and Thesis Contribution	3
1.2 Thesis Outline	5
II EXPERIMENTAL SETUP	7
2.1 Animal Preparation and Training	7
2.2 Neural Recording	8
2.3 Experimental Setup and Behavioral Paradigm	9
2.4 Data Definition	11
III VIDEO PROCESSING	12
3.1 Alignment	12
3.2 Motion parameter extraction	15
IV ARM KINEMATICS DECODING	21
4.1 Pre-processing	21
4.2 Decoding	22
V RESULTS AND DISCUSSION	26
VI CONCLUSION	36
APPENDIX A —	38
APPENDIX B —	41

REFERENCES 47



LIST OF TABLES

1	Number of usable trials for each neuron and object	16
---	--	----



LIST OF FIGURES

1	Objects and grips	10
2	Pixels average intensity	14
3	The output of motion parameters detection	18
4	Effect of hand and fingers configuration on calculating the angle . . .	19
5	Average of extracted kinematics of all of the trials and neurons	20
6	Applied pre-processing methods over raw neural data	23
7	neuron 453 decoding performance based on different pre-processing .	27
8	Mirror neurons ordered based on decoding angle using pre0-agg1 . . .	28
9	Mirror neurons ordered based on decoding angle using pre1-agg1 . . .	29
11	Non-mirror neuron 429 performance using pre0-agg1	31
12	Object based comparison of mirror and non-mirror neurons (angle) .	32
13	Object based comparison of mirror and non-mirror neurons (distance)	33
14	all-object based comparison of mirror and non mirror neurons	34
15	best-object based comparison of mirror and non mirror neurons . . .	34
16	Non-mirror neuron 449 performance using pre0-agg1	38
17	Mirror neuron 453 performance using pre0-agg1	39
18	Mirror neuron 479 performance using pre0-agg1	40
19	Mirror neurons ordered based on decoding distance using pre0-agg1 .	41
20	Mirror neurons ordered based on decoding distance using pre1-agg1 .	42
21	Non-mirror neurons ordered based on decoding angle using pre0-agg1	43
22	Non-mirror neurons ordered based on decoding angle using pre1-agg1	44
23	Non-mirror neurons ordered based on decoding distance using pre0-agg1	45
24	Non-mirror neurons ordered based on decoding distance using pre1-agg1	46

CHAPTER I

INTRODUCTION

Our brain is the main source of our actions, decisions, problem-solving strategies, emotion, etc. Understanding the underlying mechanism of brain can be very inspiring and advantageous in different disciplines such as neural prosthesis[1] and robotics[2]. The fascinating capability of brain majorly relies on its massive networks of neurons. As a very simple explanation, neurons can be seen as electrochemical cells with a threshold which receive the electrochemical signal from one or multiple neighbor neurons. If the received signal by a neuron is strong enough (passes its threshold), the neuron transmits the signal through and have the same interaction with its neighbors. Neurons are generally simplified as binary units which have state of 1 if they are passing any signal i.e. neural firing, or 0 otherwise. Brain power is the result of connection and interaction among its neurons. Understanding what the brain does, given the neural firing, which is referred as decoding problem is one of the main challenges of the interdisciplinary field of computational neuroscience. More technical definition of decoding is to model the stimuli using the brain data. The complexity and difficulty of decoding problem can be perceived by assuming the example of understanding how a computer system is running a word processor application only by having access to the pattern of varying state of its transistors[3].

In action, to capture neural data from different regions of the brain, there are multiple recording methods which are categorized into two main groups: invasive and non-invasive recording. With invasive recording, by implanting micro-electrodes inside the brain, one can capture spike occurrence of a single neuron[1]. Having recorded neural activity in the presence of predefined and measurable stimuli, the

decoding problem can be solved by a wide variety of machine learning and statistical approaches.

As mentioned at the start of this section, Brain Computer Interfaces (BMI), particularly neural prosthesis, is one of the fields that gets benefits from the discoveries made about the brain and its mechanism[1]. In the literature, studies can be found that attempted to apply the decoding paradigm for producing data to improve the development of neural prosthesis[4, 5]. Neuroprosthesis development draws more and more attention due to its potential in helping disabled people e.g. the ones who have experienced a loss of limbs or spinal cord injuries[1]. Thinking about disabilities and our daily life activities, one can not deny how the ability to move hand and arm is necessary. Loss of arm and hand movement equals to loss of being self-directed and independent in daily life[6]. According to the survey done in[7], people with spinal cord injury were asked about the ability they hope they could regain it. Regaining hand and arm function was ranked as number one among other abilities.

Majorly, we use our arm and hand to perform reach and grasp tasks. Multiple regions of our brain are involved in grasping which their homologues areas in macaques brain that have been investigated in many studies. Ventral premotor cortex, i.e. area F5, is one of these regions in a macaque monkey brain. It is proved that neurons in F5 are involved in hand movements[8]. The majority of these neurons fire when grasping is performed. However, not all of the grasping-related neurons in F5 has the same firing profile. Their neural response varies according to different factors such as required grip type, finger configuration, visibility of the target object e.g. grasping in dark or light, and action segmentation[9].

F5 area contains another group of neurons called mirror neuron which has a fascinating property. These neurons are active not only when a monkey performs a grasping task but also when the animal observes the same action being done by another subject (experimenter or another animal)[10, 11, 12]. Some studies suggested

that mirror neurons are possibly associated with action recognition in monkeys[13] and empathy in humans[14].

According to what mentioned so far, F5 becomes one of the areas of interest in the literature. There have been empirical studies with the focus on grip type classification/decoding in this area. In the following section, some of these works are introduced. The results of these studies might be useful in the neural prosthesis development for rehabilitation purposes. To the best of our knowledge, there is a lack of research on the capability of F5 area neurons in the real-time decoding of grasping details, kinematics of arm and hand during the grasping, which can be beneficial for building more realistic and practical neuroprosthesis. Moreover, there are still open questions about mirror neurons and their possible roles in motor control. In this thesis, we aim to investigate whether there are neurons in area F5 with power of real-time decoding of arm kinematics during grasping. Furthermore, how mirror and non-mirror neurons' real-time decoding power can be distinguishable. To this end, the neural activity of 32 neurons (both mirror and non-mirror) from F5 area of a macaque monkey was recorded while the animal was performing grasping. Simultaneous to the neural recording, the monkey's motion was captured with a camera. The animal's arm kinematics were extracted from videos and used to investigate whether recorded neural data can accurately decode the arm kinematics in real-time or not.

1.1 Related Works and Thesis Contribution

In the literature, there have been efforts targeting grasp classification/decoding using neural data from multiple brain regions such as ventral premotor cortex (F5), dorsal premotor cortex, primary motor cortex (M1), and anterior intraparietal cortex (AIP). These studies mostly suggest that grip classification can be done with an acceptable accuracy using neural activity of aforementioned areas. The following provides details about some of these studies. In [15] and [16], Support Vector Machines classifier is

applied on F5 neural data for decoding grip types. In [16], two sets of object were provided to the animal, and each set contained 6 different 3D objects requiring a specific grip type. One of the sets needed more advanced grasping comparing to the other set. Their result showed that 90%-95% accuracy can be achieved in predicting object types using population-level activity. Similarly, in [15], at least 96% of accuracy has been obtained decoding 6 different grips.

The work presented in [17] is also about the grip classification (4 objects with different shapes) using SVM. Whereas, the neural data used in this study was recorded from dorsal premotor cortex i.e dPM. This study revealed that information for grasp classification is available in the dPM, however, this information can be obtained right after the movement onset.

A Naive Bayesian based decoding was used in [18] for classifying two grip types and five different wrist orientations. Neural data was recorded from AIP and F5 while the monkey was grasping a bar oriented in 5 different angles by applying either precision or power grip. They reported that area F5 is the more accurate decoder for grip type while AIP is a better decoder for the grip orientation.

The provided study in [19] contains the results of target-based decoding which relies on unsorted spike trains rather than sorted spike trains. In this work, neural data is recorded as the monkey was trying to reach a target on a screen using a manipulator in front of him. This work is not much related to grasping decoding but the findings are noteworthy as spike sorting is costly in computation.

In[20], authors provide details about investigating how mirror and non-mirror neurons in area F5 are able to code self-hand visual feedback. In this study, neural recording took place in the light and dark conditions while their animal was grasping a cone shape object. Results of [20] suggest that mirror neurons show sensitivity to self-hand visual feedback during grasping the object. In [21], it has been shown that grip type prediction based on single neuron activity can be made for some of the F5

neurons.

As a recent study, [22] discusses that using population level neural activity, in addition to grip type decoding, the details of hand configuration and reaching phase can be accurately decoded. Neural data in this study is captured from M1, F5, and AIP areas while the animal was manipulating a wide range of objects. Results of this study convey that the information of decoding reaching and grasping movements is present in the mentioned area. However, F5 and M1 show higher performance in the decoding than AIP.

Most of the mentioned studies more or less reveal the possibility of grip type classification using neural activity of subsets of neurons in F5 area. Suggested decoding approaches can be used for developing neuroprosthesis to restore arm movements. But, a device with the ability to convert the brain activity to movement e.g. moving a prosthetic arm, in real-time seems more realistic and practical. On the other hand, the level of contribution F5 neurons show in the real-time decoding of arm movement can provide a new aspect to investigate the differences between neurons with and without mirror property.

In this study, we explored the single neuron power in the real-time decoding of the arm kinematics data. Recorded neurons are all from F5 including both mirror and non-mirror neurons. Then, we investigate the decoding power of both groups in a comparative way which has not been addressed in the literature to the best of our knowledge.

1.2 Thesis Outline

The thesis is organized as follows. In chapter II the experimental setup and data collection are discussed in detail. Chapter III explains how kinematics data are extracted from the videos and concurrency of neural data and kinematics data is assured. Chapter IV discusses the methods and techniques used for the decoding. The results of

the study can be found in chapter V. In the end chapter VI provides the conclusion.



CHAPTER II

EXPERIMENTAL SETUP

In this chapter, experimental scheme and data preparation are described. The whole experiment, including 25 sessions, took place in 8 days from 23/7/2015 to 11/8/2015 by Vassilis Raos and colleagues at University of Crete. During these sessions, neural activity of 44 neurons from a macaque monkey was recorded. Simultaneous to neural recording, sessions were video captured. This chapter is organized in following subsections: First subsection contains details on how the animal training and preparation were carried out. Details on how neural recording took place is provided in the second subsection. The behavioral paradigm and experimental setup are explained in the third subsection. And, the description of the data we received from the Crete lab can be found in the last subsection.

All the procedures and experiments described in this chapter were performed by our collaborators, Vassilis Raos and colleagues, at Crete University. Technical information presented in this chapter is also given to us by our collaborator. Furthermore, our project partner assured us that: All experimental protocols were approved by the Veterinary authorities of the Region of Crete and complied with the European (directive 2010/63/EU and its amendments) and National (Presidential Decree 56/2013) laws on the protection of animals used for scientific purposes.

2.1 Animal Preparation and Training

An adult female monkey (*Macaca mulatta*) was trained and involved in the experiments. An authorized supplier (Deutsches Primatenzentrum, Gottingen, Germany) purpose bred her. The first step in training is to make the animal accustomed to having a collar which is used to guide her to his seat in the experimental setup. On

the seat, except for real experiment, monkey is partially fastened to the chair in order to make the experiment secure. Whereas, during real recording, the animal is fully fixed to prevent any damage as the recording device is attached to his head. she can only move her right arm to perform the grasping.

At the early stages of training, objects are shown to the monkey. Being curious, animal tries to examine and grasp the objects. Cylinder, sphere, and ring seem more trivial for monkey to grasp. Whereas, grasping cube takes more time and effort to be fully learned by the animal. There is an LED light on objects which is used for guiding the animal during the real recording. Next step in training is that monkey needs to learn to fixate on the LED for a certain amount of time or till the moment a cue occurs. There is a window around the object to keep track of the animal's gaze. Reward is offered only if the monkey was looking at object during the fixation.

All phases of training are reward based. Whenever monkey performs a correct grip or stays fixated on LED for a desired period, she receives juice as reward. Training takes place in the morning as animal is more eager to drink. Being aware of the daily water need of monkeys, animals were offered their extra required water after the training. Moreover, lab animals are always under observation for their health to be maintained at its best condition.

2.2 Neural Recording

After training, a recording chamber was surgically implanted over the left hemisphere of the monkey. After implantation, the cortical areas accessible through the chamber were explored and localized. Area F5, the region of interest for the current study, rostral to area F4, was assessed by neurons discharge during goal-directed hand movements and observation of actions.

Glass-coated tungsten microelectrodes were used for single neuron recording. After several steps of signal processing and filtering followed by spike sorting using

Spike2 software (<http://ced.co.uk/products/spkovin>), neural activity was saved as a binary vector with 1 ms resolution.

2.3 Experimental Setup and Behavioral Paradigm

In this experiment, 4 different objects were provided to the monkey for the grasping task. Each of the objects requires its own particular grip. Objects and the needed grip are presented in the Fig.1 and explained in the following:

- Cylinder which needs finger prehension, object wrapped by all fingers other than thumb
- Sphere which needs whole hand prehension, object wrapped by whole fingers and palm being in touch
- Ring which needs hook grip, by inserting index finger in the ring
- Cube in a groove which needs advanced precision grip, object grasped by the pulpar surface of index finger and thumb being involved

These objects were placed on a rotating turntable apparatus and were shown to the animal one at a time, always in the same central position. The monkey seat was at 25 cm distance of the turntable[23].

At the beginning of each trial, an LED above the selected object turned on and the monkey had to fixate on it and press a key. Following a fixation period, a dimming of the LED signaled the onset of the reach-to-grasp movement. The monkey had to reach for, grasp, pull and hold the object while fixating on it until the turning off of the LED cuing its release. Each trial can be seen as 9 events:

1. beginning of spontaneous activity
2. object LED turns on
3. monkey fixates on the object LED

4. monkey presses the button.
5. go cue (the LED dims for a moment)
6. movement onset
7. object grasped
8. release cue (the LED turns off)
9. the object is released.

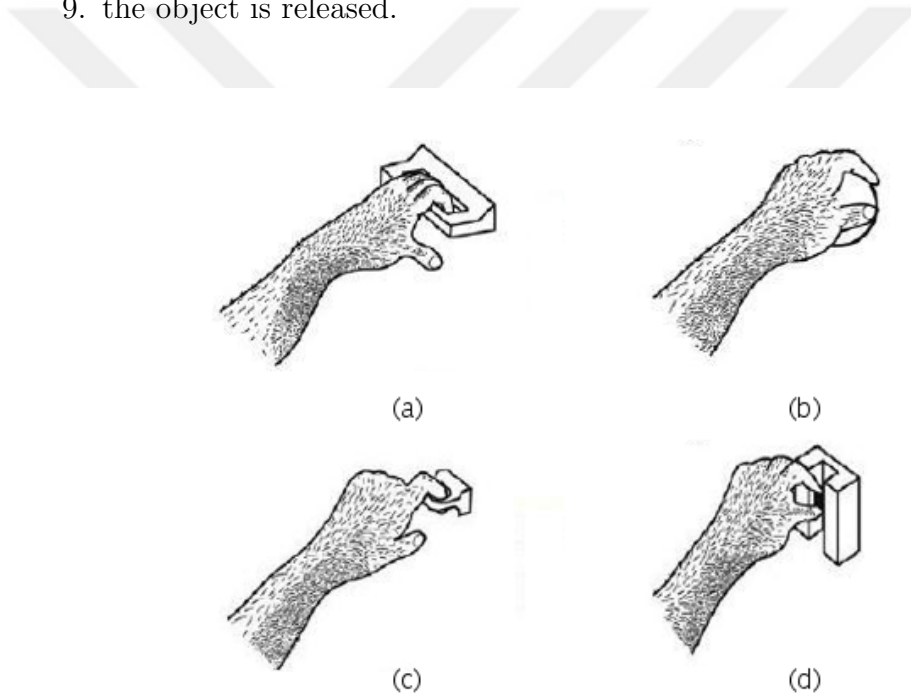


Figure 1: Objects with different grip presented to the monkey, a) Cylinder, finger prehension, b) Sphere, whole hand prehension, c) Ring, hook grip, d) cube, precision grip

The period from the start of the monkey's movement to the time of object pulling is defined as the movement epoch, 6th event. Monkey's movement was recorded at 120 frames per second by a camera that viewed the experimental setup from a constant

distance. A second LED, hidden from the monkey's view, was used to align the video frames with neural activity. This LED changed its state when the monkey's hand left the home position to reach for the object and when the object was grasped. For alignment purposes, it was crucial to robustly detect the state of this LED.

Neurons which were discharging while the grasping movements were further examined for the mirror property.

2.4 Data Definition

The Crete lab sent us two types of data which were Matlab structure files, a '.mat' file for each neuron, and video files recorded during the experiment sessions, one video file for each session. Two additional Excel files were also provided. One excel file contained information for addressing the recorded units for each video and the other carried information whether a neuron have mirror property or not.

For a particular neuron, one should refer to the Excel file to find out which video file contains the session of recording this neuron activity. Then from the neuron's structure file, following information can be extracted:

- Number of trials performed per object by the monkey
- For each trial, starting time in the corresponding video file (the reported time is not accurate enough for video and neural activity alignment)
- The time of each event during a particular trial (time origin is the advent of event 2)
- For each trial, A 5000 length Binary vector with 1 ms accuracy, each element shows whether the neuron spiked at that time interval or not.

CHAPTER III

VIDEO PROCESSING

This chapter explains how the kinematics data is extracted from the video files and how the alignment of derived kinematics and neural data is achieved. It is very crucial for the neural data and kinematic data, extracted from the video files, to be synchronous in order to achieve reliable decoding results. The following section contains details on alignment of the data from videos and neural activities. Later, the method used for kinematics data extraction from video files is explained.

3.1 Alignment

Extracting the video frames corresponding to each trial is the first step in data alignment. As mentioned before, during a trial, the monkey was performing the grasping in a predefined set of events, nine in total. These events cover moments before monkey fixates on the object till the moment the animal releases the object. Throughout a trial, although the brain activity may vary, the monkey is physically motionless except during movement epoch i.e. event 6. Therefore, motion parameters should be extracted from the frames which are concurrent with this event. As stated earlier, there is an LED which the monkey has no hint about. The purpose of this hidden light is for synchronizing the neural activity with corresponding video frames.

The LED can have two states of being on or off and it switches between the states depending on the animal movement. From the start of a trial till the 6th event onset, LED stays off. When animal releases the home position, it turns on and remains on until the moment the object is grasped. While the animal is holding the object, the LED stays turned off. Next switching happens as the object is released and the hand is moving back to the home position. In short, during a trial, LED switching happens

twice. Both times are when the arm is moving and not placed on home position or the target.

It is crucial to detect the first switching in order to extract exact concurrent frames of the movement epoch. For the detection, changes in average pixel intensity were measured in the rectangular area of frames which holds this LED. In the next step, by using semi-manual filtering, frames in which the LED switches from on to off or vice versa were found. The synchronous video frames of a trial for a particular neuron and object were obtained following these steps:

1. Given a neuron, deriving the related video file using the Excel file
2. Extracting the approximate start time of the trial in the video file using information in the neuron's Matlab structure file.
3. Starting from obtained time in the previous step, Looking at frames for detecting the one frame in which second LED switching happens (This frame is concurrent with the advent of event 6.)
4. Keep saving frames until the frame in which second LED turns off.
5. Storing the frames in a file with a distinct name comprising neuron's, object's and trial's information

Described steps can be explained simpler by looking at Fig.2. In the figure, pixel intensity measurement can be seen in a video file. Blue and red plots depict pixels value and our filtering result respectively. None of these plots are perfect near to the end because of the noise in the captured videos. For a given trial, one should first extract the approximate start time of the trial (step one), next finding the corresponding frame on the horizontal axis. The first rise in the red plot after the found frame point is the onset of movement epoch for the given trial.

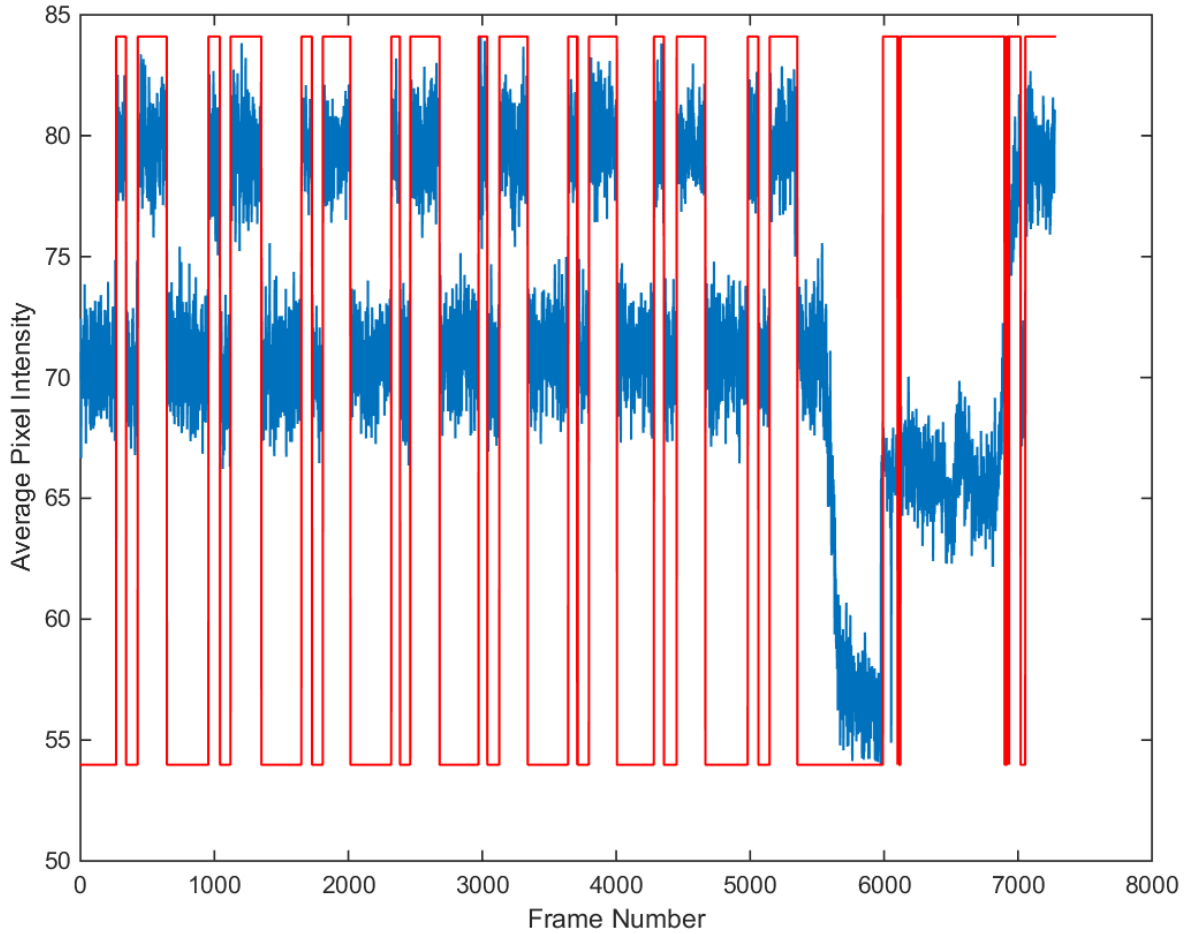


Figure 2: Changes in average pixel intensity in the rectangular area containing the LED, blue plot shows the intensity for each frame and red plot is the filtering result

As mentioned above, all the valuable changes (grasping action) occur during the first switching of the LED. Therefore, it is critical to be assured that first and second switching are not confused in the detection. Sometimes, due to the noise in videos, it was impossible or time consuming to detect the LED state. Another problem faced was that the starting time in the '.mat' file was overlapping with the finishing of the previous trial i.e., the second on-off state of the LED. This made the approximation of the starting time of a trial erroneous almost fifty percent of the times. Unfortunately, the noise effect was unavoidable. But, for the later problem, frames of both on-off

phases of the LED has been extracted and saved to different files. Video files showing meaningful grasping action were separated manually. Due to these problems some trials were eliminated from the analysis. As a final result, the number of usable trials in the analysis became fewer than the performed trials even dropping to 6 out of 10 in some cases.

One negligible error for some neurons was that the given times for a particular object were not directly mapped to that object. This problem caused to eliminate some of the trials or the neuron entirely from the analysis. Table 1 shows the number of usable trials for each neuron and object. Neurons with 0 trials for all objects were eliminated from analysis due to noise or error in the data. In the end, for each valid trial, there is a video file named in a descriptive way showing neuron and object that the trial is related.

3.2 Motion parameter extraction

So far, a separate video file is available for each valid trial. As the camera had been located at the same point during the whole experiment, the physical measures of the setup and pixel scale conversion can be done consistently for all the video frames. For more accurate result, the coordinates of the monkey's wrist at home position and the center of objects have been marked manually in the frames related to each object. These coordinates can be used to define the sub-area of the frames where the action happens. A set of image processing methods was applied on the extracted sub-area. Two parameters of arm motion could be calculated consistently for each frame in a trial: the approximate position of the wrist and the angle of the monkeys arm with the axis parallel to his body. The latter is the summation of two angles which shoulder and elbow joints make to perform the action. These two kinematics values, henceforth are called as angle and distance. Following steps were applied on the extracted sub-area to obtain motion parameters:

Unit No.	Cyl.	Sph.	Ring	Cube	Unit No.	Cyl.	Sph.	Ring	Cube
423	0	0	0	0	437	0	0	0	0
424	0	0	0	0	438	0	0	0	0
426	20	17	10	10	441	9	7	7	8
427	20	17	10	10	446	7	6	6	10
428	20	19	9	10	447	7	7	7	9
429	20	19	9	10	448	7	15	6	9
430	8	8	7	8	449	7	15	6	9
431	8	8	7	8	450	0	0	0	0
434	0	0	0	0	451	8	17	7	9
435	13	14	8	10	452	8	17	7	9
436	0	0	0	0	453	9	8	9	8
437	0	0	0	0	454	9	8	9	8
438	0	0	0	0	455	6	9	9	8
441	9	7	7	8	456	0	0	0	0
446	7	6	6	10	457	10	10	10	10
447	7	7	7	9	458	10	10	10	10
448	7	15	6	9	459	8	10	10	10
449	7	15	6	9	463	9	9	9	10
450	0	0	0	0	470	0	0	0	0
451	8	17	7	9	471	0	0	0	0
452	8	17	7	9	472	10	10	10	10
453	9	8	9	8	473	20	10	17	10

Table 1: Number of usable trials for each neuron and object

1. Applying MATLAB ForegroundDetector from computer vision toolbox to get a mask for each frame showing the moving pixels.
2. Using different filters to reduce noise as much as possible without losing the integrity of the pixels of the arm.
3. Assigning time profile for components defined by moving pixels (noises from level 2 can be large enough to affect the kinematics extraction negatively. These noises can be caused by brief jerks that happen in the parts of the setup connected to the monkeys seat as monkey eagerly wants to grasp the object. This kind of noises may be large, but they are short in duration. So, by assigning time profile for each component of the mask, these sudden jerks can be detected.)

4. Using `canny` (for edge detection), `findContour`, and `minAreaRect` tool from OpenCV to obtain the motion parameters

Fig.3 shows a frame corresponding to sphere object grasp. It can be seen that all unwanted noises are eliminated and only arm pixels are detected as the main moving component. The bold gray rectangle in the figure is the selected sub-area of frames where motion happens. Points marked by green, blue, and red colors are the center of the object, home position of the wrist and monkey's shoulder respectively. The other rectangle, in the figure, is the output of `minAreaRect` tool from OpenCV which is used to extract the kinematics data. The lower edge of `minAreaRect`, blue edge in the figure, was used to define the angle lower arm makes with the vertical axis. The wrist position is estimated as an average of pixel positions which were located in 15% of the `minAreaRect` area at the ending near the object.

We faced some challenges during the kinematics extraction using `findContour` tool of openCV which is worthwhile to mention. Although the input image for `findContour` was a clean frame out of noise only containing arm pixels as a single component, the output was a composition of several distinct contours. It was happening because of the effect of edge detection needed before. Having a fully connected contour outlining the arm's pixel is very necessary for the `minAreaRect` tool.

Another problem encountered was the effect of hand configuration on calculating the angle. As shown in the Fig.4, by fingers placing lower than the arm, the rectangle covering whole hand and arm can't be used as correct reference for the angle. In order to overcome this problem, we masked half portion of the available pixels at the object side (where pixels related to hand are present), then we repeated the same procedure by applying `findContour` and `minAreaRect`. The result is the green rectangle shown in Fig.4.

In spite of our hope, no details about hand shaping or finger aperture were extracted from the videos. Obtaining more kinematics details were impossible because

of two reasons. First, we were limited to a 2D lateral view of the action with no marker on the wrist or critical joints. Second, FPS (frame per second) of the camera seems to be not enough to capture monkey's fast motion. Consequently, the captured frames were blurry at the fingers and it was impossible to achieve more details. Another option for future research can be instead of having only one object representing a grip type, multiple objects with different sizes be included for each grip category. In this way, considering the smallest object as a baseline, a proportional factor of hand shaping or finger aperture can be estimated by pixel-wise comparison.

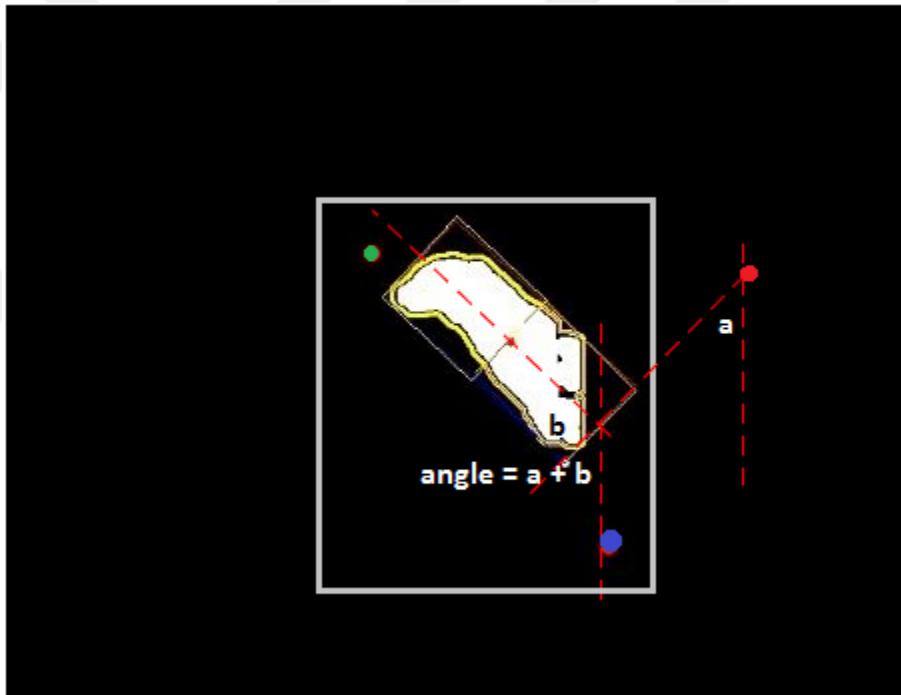


Figure 3: The output of motion parameters detection

Trials were different in length even within the ones related to a single object and neuron. For the convenience in the decoding, for each neuron, it was desired that trials related to a single object have the same length. Therefore, for each trial, some starting and ending frames were neglected.

At the start of each trial, there is no arm movement (no changes in wrist position) and monkey spends some time to shape his hand. Some frames after the movement

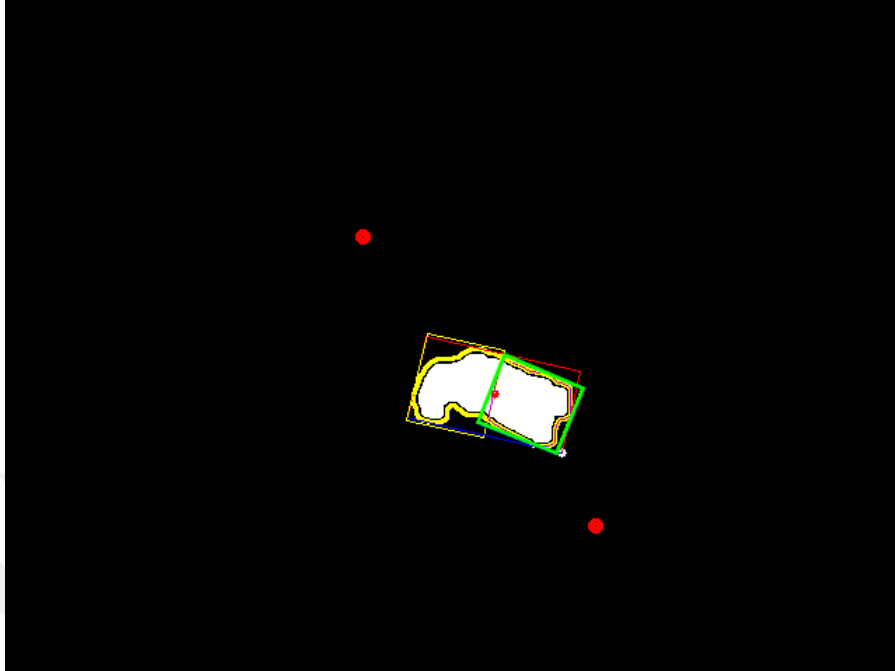


Figure 4: Effect of hand and fingers configuration on calculating the angle

onset, the monkey starts to move the arm towards the target. As mentioned earlier, motion parameters extracting method is only able to obtain information of lower arms angle and approximate wrist position. Therefore, for early frames, there is no value for the kinematics parameters. These frames have been neglected from the beginning of a trial until the first frame with meaningful value for lower arm.

A partially similar thing happens for the ending frames where monkey spends time on placing the hand on the object, tightening his grip, and completing the task. Therefore, there is no movement of the arm and wrist anymore. This time, motion parameters extracting method generates constant values for the kinematics data. These frames with repetitive data are also neglected from the end of the trials. After shortening the trials from head and tail, if a neuron still contains trials with different length for a single object, then these trials are cropped further from the end to become equally long as the shortest one.

In order to avoid losing the concurrency of video data and neural activity, the number of neglected frames was saved. Valid frames were numbered considering the

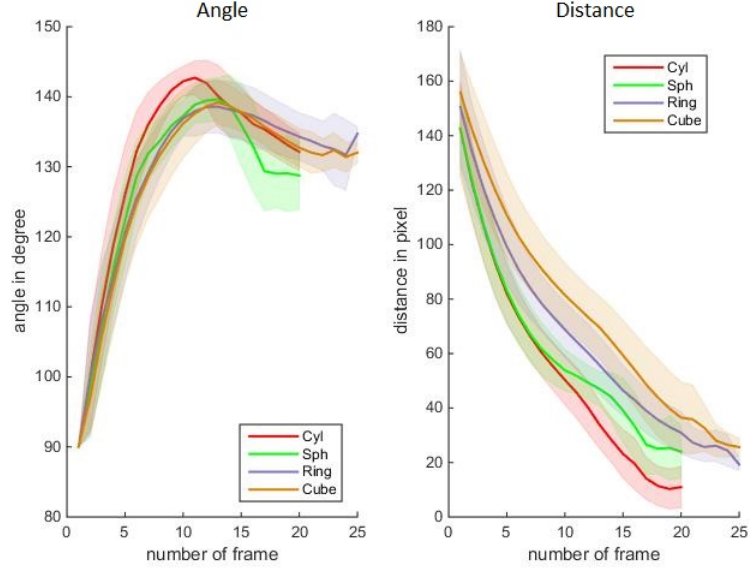


Figure 5: Average of extracted kinematics of all of the trials and neurons

count of skipped frames. By using frame rate of the video, these numbers were converted to time and summed with the event 6's onset time. Using Eq.1, for each data point in the kinematics array, corresponding time index in the neural firing array is calculated and saved along with the kinematics array. In the mentioned equation, t_{fr} , FPS , fr_{no} and t_{onset} are time index of a frame, frame rate of the videos, number of the frame counted from movement onset and time index of the movement onset respectively.

$$t_{fr} = \frac{1000}{FPS} fr_{no} + t_{onset} \quad (1)$$

As a conclusion, for each trial, an array of kinematics data and corresponding time index were generated. Due to the mentioned limitations, these data don't cover the 6th event entirely. Instead, they cover the movement event from the moment that the monkey's arm appears in the scene (after achieving initial hand configuration) to the time the object is reached but not fully grasped.

Fig.5 summarizes the output of kinematics extraction for both angle and distance. Each curve shows the average of kinematics data over all the trials for a particular object. Shaded area around the curves depicts the corresponding standard deviation.

CHAPTER IV

ARM KINEMATICS DECODING

In order to find out whether the neural activity can decode kinematics data or not, linear regression was used. Before going into the decoding details which is provided in the last part of this chapter, suggested pre-processing approaches applied on neural spike train can be found in the following section.

4.1 Pre-processing

The first step in pre-processing of neural activity was to convert neural spikes into a continuous signal. Sliding windows with Gaussian convolution over each window has been used. Width and center point for each window considered as 50 ms and the time index corresponding to each data point in the kinematics array, respectively. One-third of the window's width was selected as the variance for Gaussian. Over each window, first, a Gaussian was placed. Then each Gaussian was multiplied by the number of spikes in the corresponding window. As windows were overlapping, the final signal was the summation of all windows (Fig.6(b)).

Once the continuous signal was achieved, the neural activity values for time indexes of kinematics data were extracted. As a result, for every trial, there was a kinematics array with a corresponding activity array of the same length extracted from the continuous signal.

Two more levels of pre-processing were applied after extracting the continuous signal. One of them was to aggregate the continuous signal by time, and the other was to include the neural activity, which happened before the movement event, into the continuous signal.

One can presume that the signal (described in the beginning of this section) during

the movement is driving the monkey’s arm while grasping. As this is a plant with non-negligible dynamics, for running the arm, it is reasonable to assume that a neural activity at a given time is not only effective instantaneously, but it also has its impact on the future. Therefore, at each point in time, in addition to the current activity, past activities are also taken into account in a decaying manner. The decaying manner means the current time gets affected more by nearly occurred activities than further activities in time. We modeled the decaying factor as an exponentially descending function which starts from 1 and gradually decreases to 0, $e^{-\frac{t}{0.2}}$. Fig.6(b) represents the explained procedure. The top subplot shows the spike rate as a continuous signal. At each point in time (time points correspond to video frames), the signal value is multiplied by the decaying function which is shown in the middle subplot. The final version of the signal is the aggregation of all these descending functions multiplied by the corresponding neural activities (Last subplot in Fig.6(b)).

In order to contribute the activity that a neuron illustrates before the movement epoch in the decoding, brief information as a summary of the activity before movement onset is concatenated with the signal. This information is simply firing rate (the number of spikes divided by duration in ms) during each event before event 6. As mentioned, motion parameter detection approach was unable to capture kinematics data for some time at the beginning of the event 6. The uncovered interval of event6 onset was assumed as event five continuation. As a result, 5 discrete values were concatenated to the signal.

4.2 *Decoding*

Polynomial family is considered as a candidate model for the decoding. In order to solve the decoding problem, linear regression with pseudo-inverse solution was used. Input and output for the linear regression were pre-processed neural signal and kinematics data respectively. According to the pre-processing approaches explained

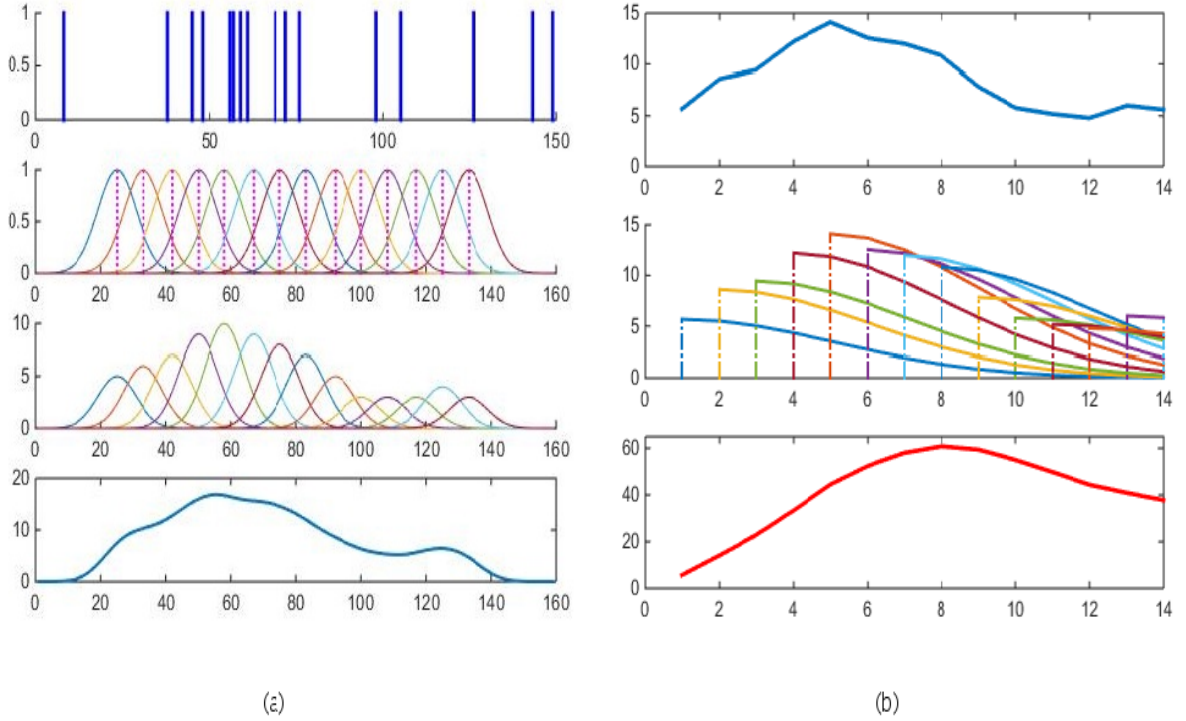


Figure 6: (a) Gaussian convolution of neural spike count, from top: Neural spikes, Gaussian of each window, Multiplied Gaussian by the spikes counts, Continuous signal (b) Aggregation of the continuous signal by time, from top: Continuous signal, Consideration of decaying effect at each time point, Aggregated signal

earlier, there were 4 possible ways to prepare the input for the linear regression.

Regression input data can be extracted from:

- 1. convoluted spike count
- 2. aggregated signal with decaying effect
- 3. the convoluted spike train concatenated with pre-movement activity information.
- 4. aggregated signal after applying decaying signal concatenated with pre-movement activity information. Henceforth, these approaches are referred as pre0-agg0, pre0-agg1, pre1-agg0, pre1-agg0 respectively. agg1 or agg0 means whether convoluted spikes count signal is aggregated or not. The Same logic

works for pre1 or pre0 which indicates whether pre-movement data are concatenated to the signal or not.

Angle and distance are two available kinematics data to be used separately as regression output. For each neuron, linear regression was solved for 32 times considering all 4 objects, 2 type of kinematics data and 4 possible ways to provide neural activity as regression input.

As mentioned above, polynomial based model with linear regression solution was suggested for the decoding. Based on a cross-validation result, polynomial with degree 2 was selected as a suitable model. The derived model for pre0-agg0 and pre0-agg1 inputs is defined with 3 parameters which can be seen in Eq.2. In the equation, $W_{1...3}^D$ refer to model parameters corresponding to distance kinematics decode and $W_{1...3}^A$ refer to model parameters corresponding to angle kinematics decode. S can be either pre0-agg0 or pre0-agg1. Like the kinematics type, the choice of signal type also leads to a different model.

$$\begin{aligned}
 Distance(t) &= W_0^D + W_1^D S(t) + W_2^D S(t)^2 \\
 Angle(t) &= W_0^A + W_1^A S(t) + W_2^A S(t)^2
 \end{aligned}
 \tag{2}$$

For more augmented inputs which contain pre-movement information(pre1-agg0 and pre1-agg1), regression model needs 5 extra parameters which is shown in Eq.3. In this equation, $W_{1...3}^D$ and $W_{1...3}^A$ are same as Eq.2. $\omega_{1...5}^D$ and $\omega_{1...5}^A$ refer to the model parameters corresponding to the pre-movement information. Pre-movement information, as mentioned, is the number of spikes a neuron generated during each event before movement onset- event 6. In the equation, $Ev_{1...5}$ represents the number

of generated spikes during events 1 to 5.

$$\begin{aligned}
Distance(t) &= W_0^D + W_1^D S(t) + W_2^D S(t)^2 + \omega_1^D Ev_1 + \omega_2^D Ev_2 + \\
&\quad \omega_3^D Ev_3 + \omega_4^D Ev_4 + \omega_5^D Ev_5 \\
Angle(t) &= W_0^A + W_1^A S(t) + W_2^A S(t)^2 + \omega_1^A Ev_1 + \omega_2^A Ev_2 \\
&\quad + \omega_3^A Ev_3 + \omega_4^A Ev_4 + \omega_5^A Ev_5
\end{aligned} \tag{3}$$

As stated in the previous chapter, the number of valid trials among all neuron and object combinations varies between 6 to 20. The difference in the number of available trials was moderated by involving at most 10 trials for each neuron and object. This deduction seemed necessary to guarantee statistical fairness. Selected trials should be distributed in two groups: train and test. Train group members define the model and generate training error while test members assess the suitability of the calculated model and produce test error. Train and test errors are defined as mean squared error. Because of the high variance in neural activity among the trials of a single neuron and object, it is safer to have all the trials contributed in the train and test phase of regression. Therefore, as a perfect option, leave one out or also known as LOO, was used to determine the test and train members. LOO approach, in an iterative manner, leaves one trial out and uses the remaining to solve the regression problem and later uses the left out trial to test the defined model. At the end, training error and test error are reported as an average of training and test errors of each iteration. The final model also is an average of the models obtained in each iteration.

Obtained LOO test error is considered as measure of neurons' performance in the decoding.

CHAPTER V

RESULTS AND DISCUSSION

In this section, the results of the last step, decoding kinematics data using neural activity, are visualized and interpreted considering different aspects of the problem. As mentioned, for each neuron, linear regression was solved 32 times considering all 4 objects, 2 types of kinematics data and 4 possible ways to provide neural activity as regression input. This variety makes possible multiple directions from which to explore the results. The effect of each factor (kinematics type, object, neuron type and pre-processing of the spike train) can be visualized and analyzed separately or in combination. The criteria of comparison and evaluation is based on single neurons decoding performance in the kinematics decoding (LOO test error).

We examine the signal pre-processing effect at first. Having pre0-agg0 as input, the regression did not perform well, and it simply generated an approximately constant line which is equal to the average of real data. On the other hand, feeding aggregated signal, pre0-agg1, as regression input improves the decoding performance considerably and generates output curve with a better approximation of real data. The results also suggest that feeding pre1-agg0 and pre1-agg1 as regression input causes obvious overfitting or makes no difference at all comparing to pre0-agg0 case.

Fig.7 presents the decoding result for neuron 453 for a single object, cylinder, but different signal preparation. Every subplot provides corresponding data in the form of shaded curves. The leftmost column is related to pre0-agg0 input, and it is followed by subplots related to pre0-agg1, pre1-agg0 and finally, pre1-agg1. In the figure, neural activity, the result of decoding angle, and the result of decoding distance can be seen in the first, second and third rows respectively. The curves are

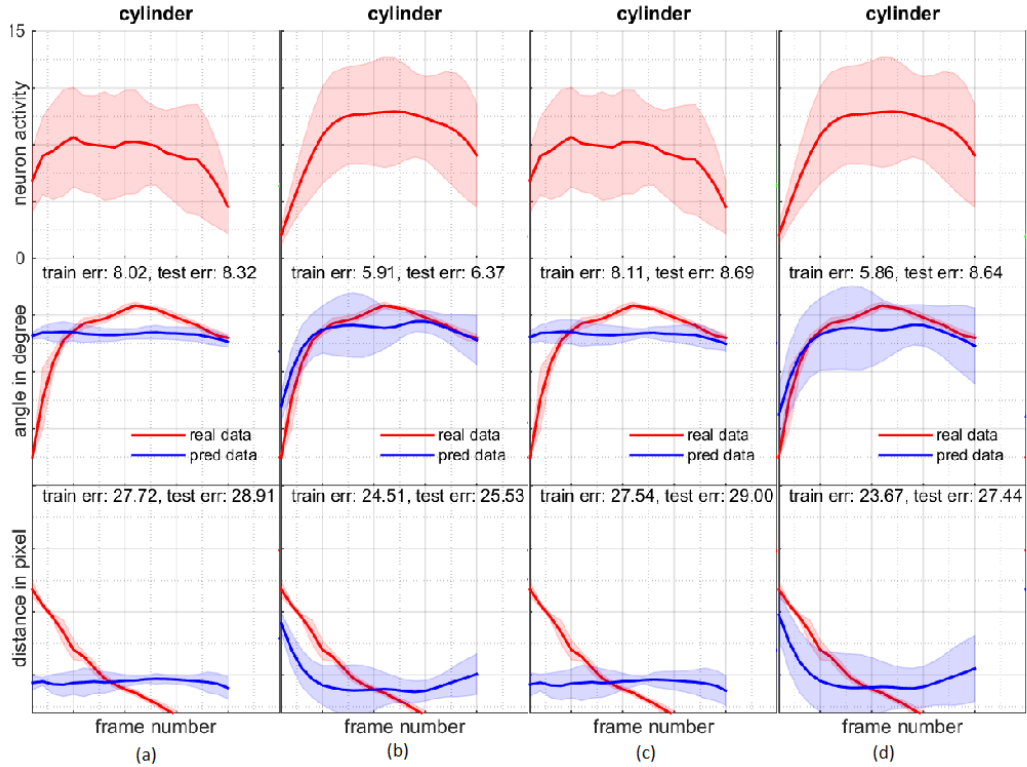


Figure 7: neuron 453 performance as average \pm standard deviation over all the trials for cylinder object and different inputs, the first row is the average of the aggregated neural activity, second and third rows represent angle and distance respectively: blue curve is the average of extracted kinematics and the red curve is the average of the corresponding predicted kinematics.

the average, and the shaded regions are the standard deviation of all the trials. This plot clearly shows that pre0-agg1 and pre1-agg1 are wise choices to be given as input for decoding.

Fig.8 and Fig.9 support the selection of pre0-agg1 over pre1-agg1 which will be helpful for further investigation by narrowing the results. In order, Fig.8 regards to the mirror neurons' performance in decoding angle with pre0-agg1 input and the mirror neurons performance in decoding angle with pre1-agg1 input. In these figures, neurons' performances are provided for all objects in a sorted manner. Training and test errors regarding each neuron can be seen as two adjacent bars with different shades. By observing these bars, overfitting can be seen clearly in the plots related

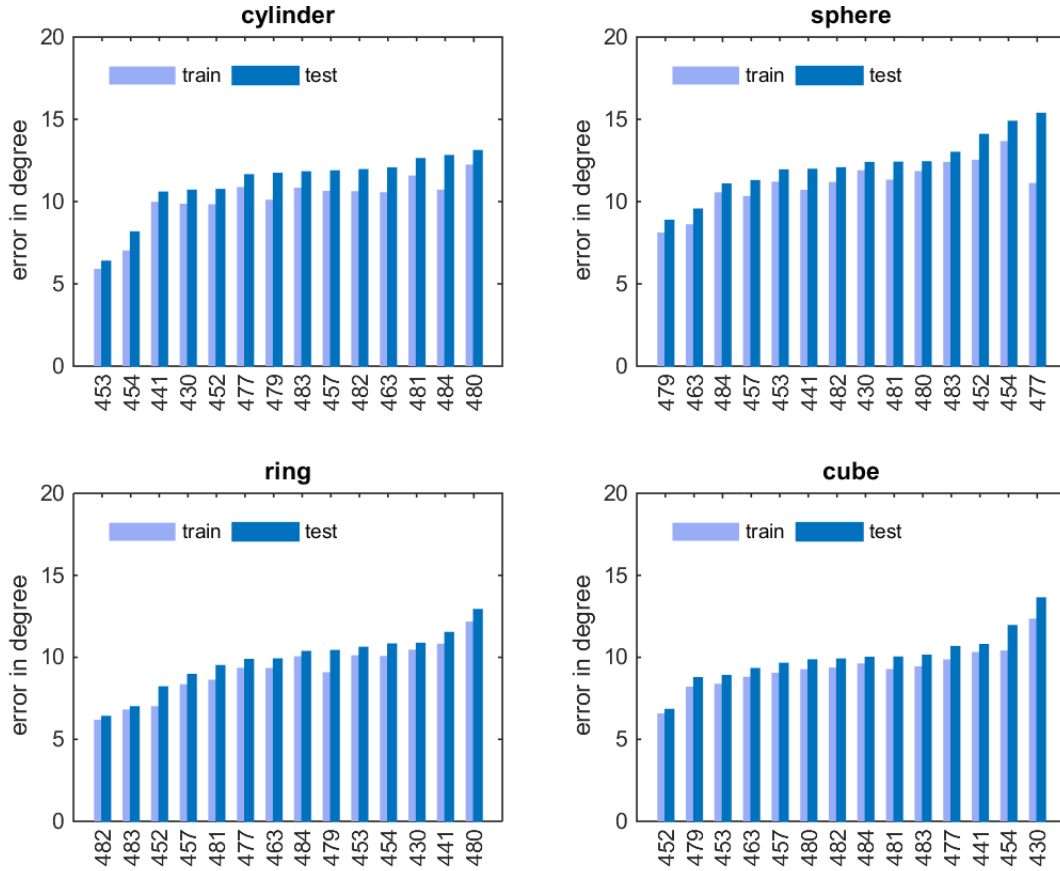


Figure 8: List of neurons ordered based on their performance (test error) in decoding the angle data required for each object by using pre0-agg1 input, neurons number on horizontal axis

to the decoding with pre1-agg1 input specifically at the end of the list. Same plots related to non-mirror neurons and distance decoding can be seen in the appendix 2.

In Fig.11, the decoding results related to neuron 429 using the pre0-aqq1 input, are presented. Similar figures for some other neurons can be found in appendix 1, Fig.16...18. These figures are similar to Fig.11 in all aspects except for what they represent in the columns. Each column, in Fig.11...18, is related to a particular object. What was mentioned so far shows that an admissible kinematics decoding using single neuron activity (using pre0-agg1,) is possible. This leads us to further investigation in the results which is the comparison between mirror and non-mirror neurons.

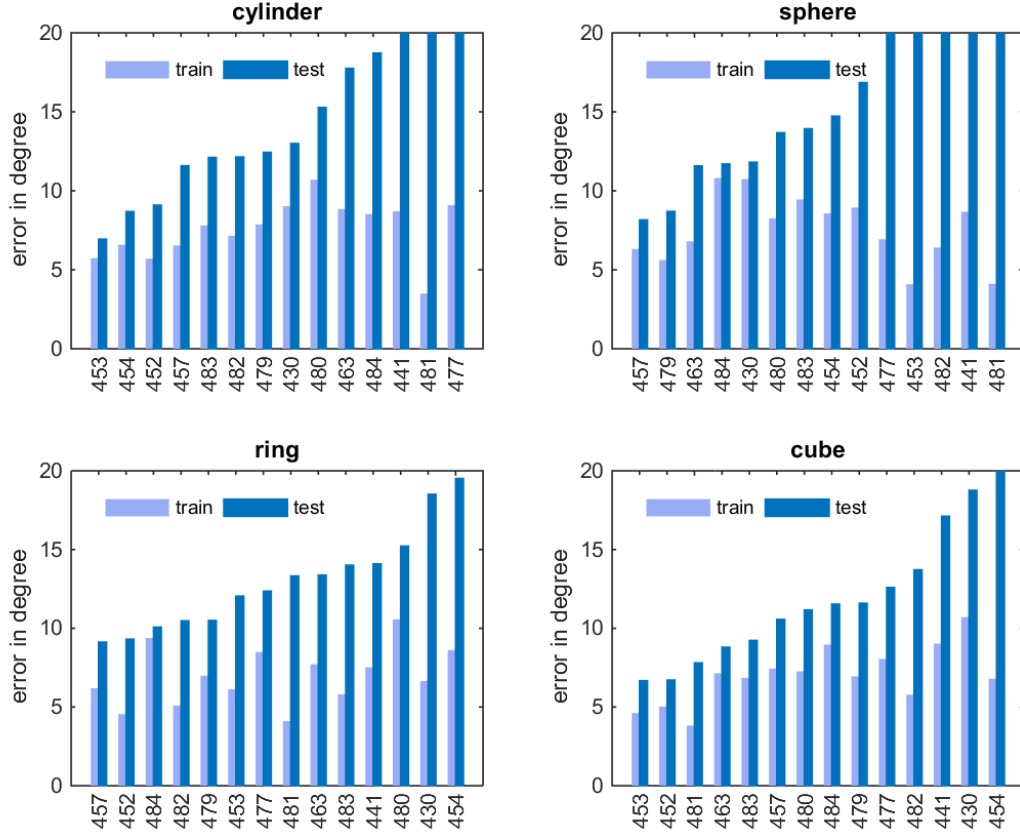


Figure 9: List of neurons ordered based on their performance (test error) in decoding the angle data required for each object by using pre1-agg1 input, neurons number on horizontal axis

Fig.10 summarizes the result in most aspects. Each neuron can be seen as a point based on its decoding performance of both kinematics data. Red points and blue points are showing non-mirror and mirror neurons respectively. Each subplot stands for a specific object. These plots can be an intuitive way to see whether or not any separation based on decoding performance can be found between mirror and non-mirror neurons. Neurons can be separated by considering both kinematics decoding results or each kinematics data individually. In order to observe neurons performance on single kinematics data decoding, one can envision each point projection on the related axis. Two things can be concluded from Fig.10: First, mirror and non-mirror neurons performance may be distinguished considering specific object or kinematics.

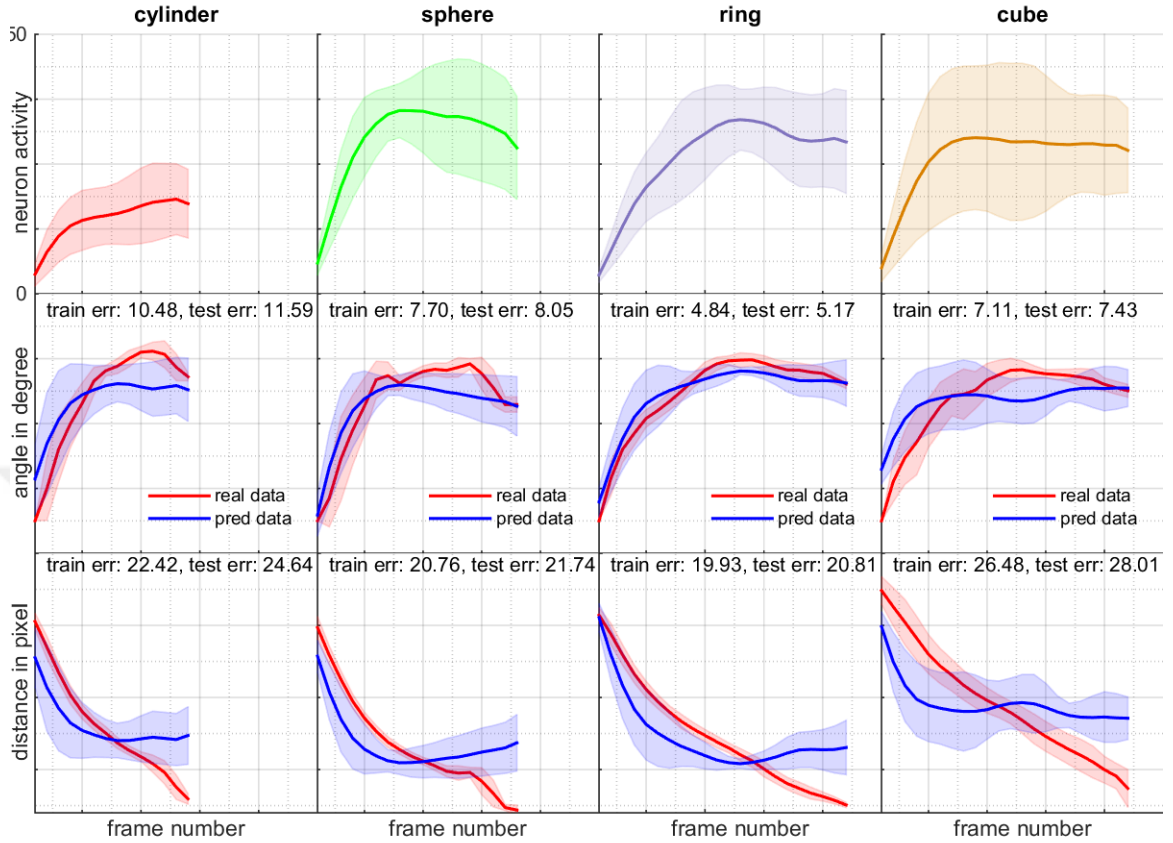


Figure 11: non-mirror neuron 429 performance as average \pm standard deviation over all the trials for each object: the first row is the average of the aggregated neural activity, second and third rows represent angle and distance respectively: blue curve is the average of extracted kinematics and the red curve is the average of the corresponding predicted kinematics.

respectively. For a valid statistical comparison, T-test with 0.05 significance level is practiced. Moreover, for each comparison, the corresponding p-value can be seen on top of each compared bars. If the difference is significant, then corresponding pairs are marked with '*'. From the recent plots, no solid or consistent conclusion can be interpreted. This can be because of the small size of each group population. On the other hand, some neurons might be object-selective or non-selective at all (general decoder). Although subplots in Fig.12 and Fig.13, are object based, object selectivity of neurons has no reflection in the plots. If a neuron is object-selective it will have higher decoding performance regarding that specific object, but, still, same neurons

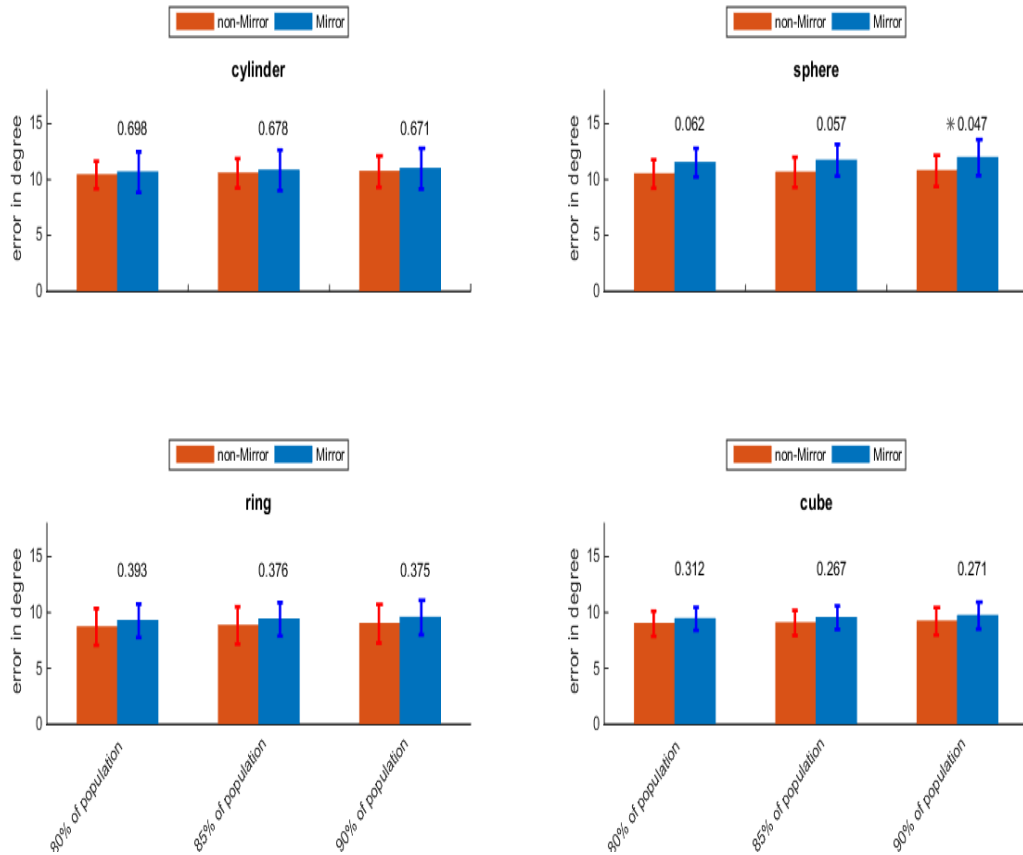


Figure 12: Comparing mirror and non-mirror neurons performance in decoding angle data required for each object

performance has been taken into account in other subplots related to other objects. In simpler terms, if a mirror neuron is a good decoder for angle decoding of a cube, it will raise the average performance of mirror groups for angle and cube. On the contrary, the same neuron will cause a drop in the average performance of mirror groups considering other object and kinematics data.

In order to overcome stated issues, two alternative methods were defined for comparing the neural groups. The first method is named all-object error which is the average value of decoding errors of all objects. The second method is named best-object error which is the minimum value of the generated decoding errors among all objects.

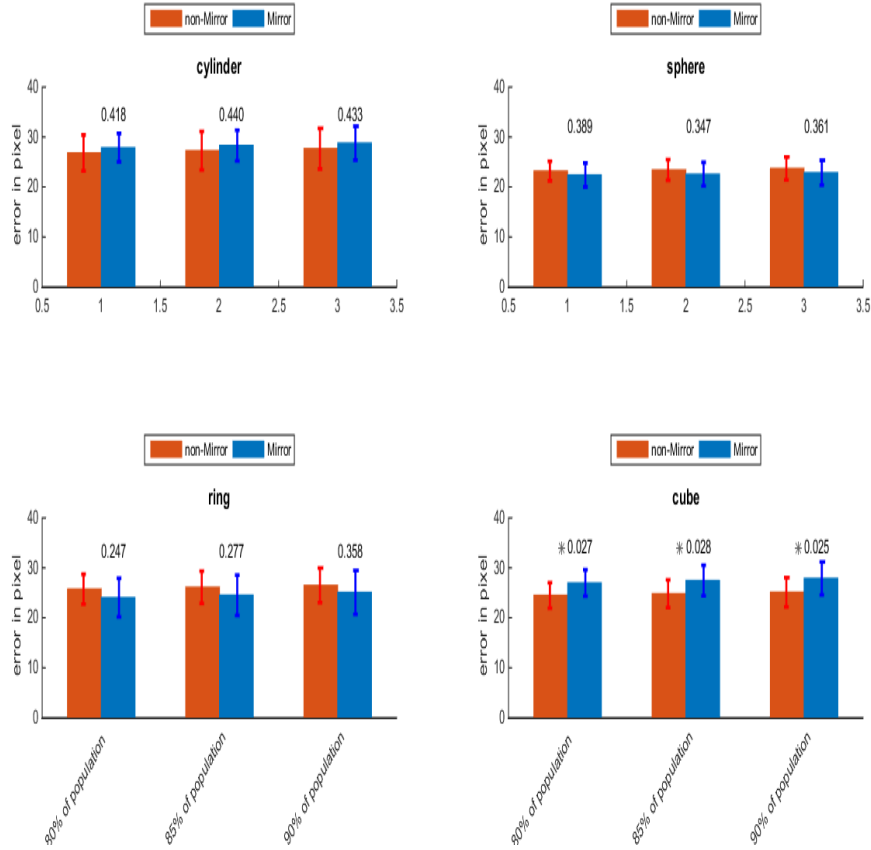


Figure 13: Comparing mirror and non-mirror neurons performance in decoding distance data required for each object

Fig.14 and Fig.15 summarize decoding results for mirror and non-mirror neurons considering both kinematics. Vertical axis shows all-object decoding error in Fig.14 and best-object decoding error in Fig.15 respectively. For each mirror and non-mirror group, reported all-object/best-object error is the average of corresponding error of the neurons in the respective group. Same as Fig.12 and Fig.13, horizontal axis of subplots represents the number of included neurons of each group in percentage (80%, 85% and 95% percent of each population). Similarly, t-test with 0.05 significance level is applied to determine the differences. And, the p-value of compared bars is shown in the plots. * is used to mark the pairs with a significant difference.

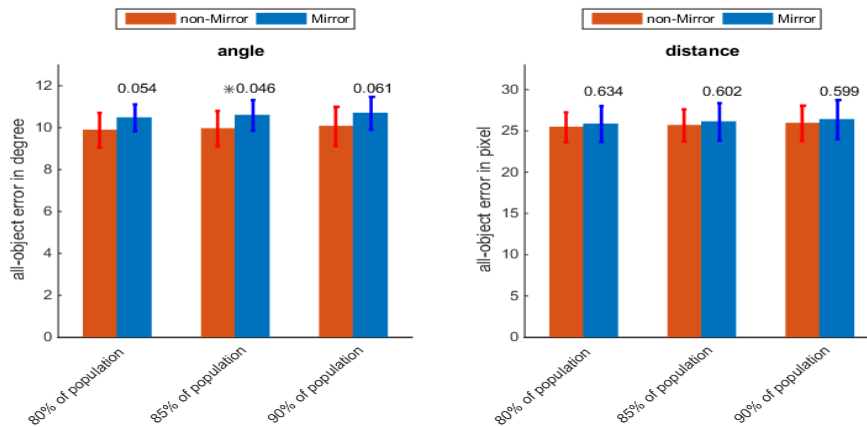


Figure 14: Comparing mirror and non-mirror neurons decoding performance based on mean all-object prediction error for each group

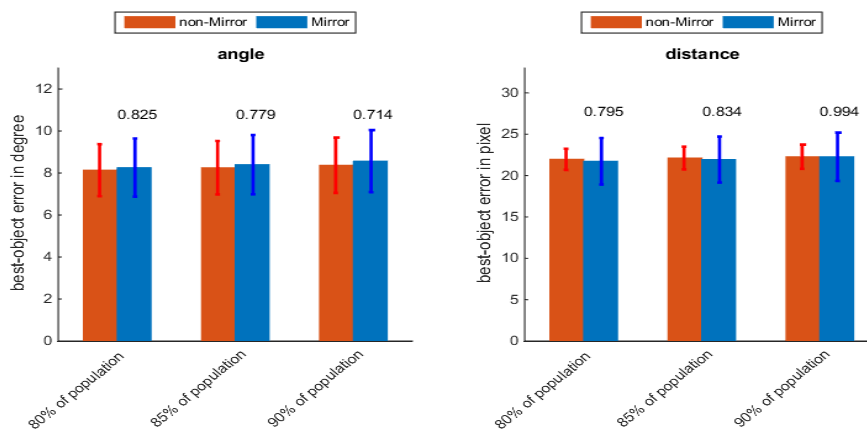


Figure 15: Comparing mirror and non-mirror neurons decoding performance based on mean best-object prediction error for each group

Non-mirror neurons seem to be better decoders than mirror neurons when evaluation of neurons' performance is carried out based on all-object error. And, by focusing on angle kinematics and involving 85% of each population, non-mirrors becomes significantly better decoders. In contrast, the comparison based on best-object error shows no significant difference between mirror and non-mirror neurons. However, in some cases, slightly mirrors seem to be a better decoder. These results suggest that non-mirror neurons appear to be better general decoders whereas mirror neurons

seem to be more object specific decoders.



CHAPTER VI

CONCLUSION

In this thesis, arm kinematics decoding of a monkey while grasping is investigated using neural activity . The activity of 32 neurons from F5 area of a macaque monkey was recorded while the animal was performing grasping tasks. Four objects, each requiring a distinct grip type, were provided to the monkey. Simultaneous to neural recording, the activity of monkey was video captured in order to extract arm kinematics detail. Steps taken for this work are as following. First, we tried to obtain synchronous frames with each trial. Second, kinematics data was extracted from the frames. Although we could extract only two kinematics elements, our plots showed us extracted data are distinguishable for each object. In the last step, we tried to solve the kinematics data decoding problem using concurrent neural activity.

For the decoding, we focused on single neuron and regression based decoding. Concurrent neural activity with the movement epoch and kinematics data were used as regression input and output respectively. Four different preprocessing approaches were carried out on raw spiking train, and decoding problem was solved by considering degree 2 polynomial as a model for decoding. Results show that single neuron decoding of kinematics data is possible with aggregated neural signal over time as input. It was not far from our expectation that the animal arm which is a dynamical system might be more compatible with the aggregated input. Decoding results were satisfying as the plots in Appendix A show that despite the high variance in the neural activity through the trials, decoding output (prediction data) is robust and reliable. Therefore, the performance of the decoding (decoding test error) was used as a metric to compare mirror and non-mirror contribution in kinematics formulation.

In this study, four different objects were provided to the monkey to grasp. Each object has its own affordance. The extracted kinematics data reveal that the animal takes shorter time to grasp cylinder and sphere in comparison to other objects. Moreover, the curves depicting kinematics data of cylinder and sphere look similar. On the other hand the curves related to ring and cube look like each other as well. Based on these findings, objects can be categorized in two sets. Although, we were expecting that mirror and non-mirror neurons decoding power will be distinguishable for these two sets, object-based analysis on the results of the decoding did not reveal any consistent differences except for two cases. The first case was decoding angle for object sphere and the second case was decoding distance for the cube. This can be the side effect of our small sample size or other factors which need more investigations.

As another option for comparing mirror and non-mirror neurons decoding power, we defined all-object error which is the mean of decoding errors over the objects. In this case, non-mirror neurons become significantly better decoders in decoding angle when 85% of each population were included. This shows that non-mirror neurons are likely better general decoders. Therefore single-neuron decoding capacity may be used as a quantitative means to classify neurons in a given region.

Although main line view on mirror neurons favors that they are involved in high-level cognitive function such as intentions encoding, we found that some mirror neurons may encode low-level motion features. Investigation with more neurons and better motion capture system is needed to support the current results.

APPENDIX A

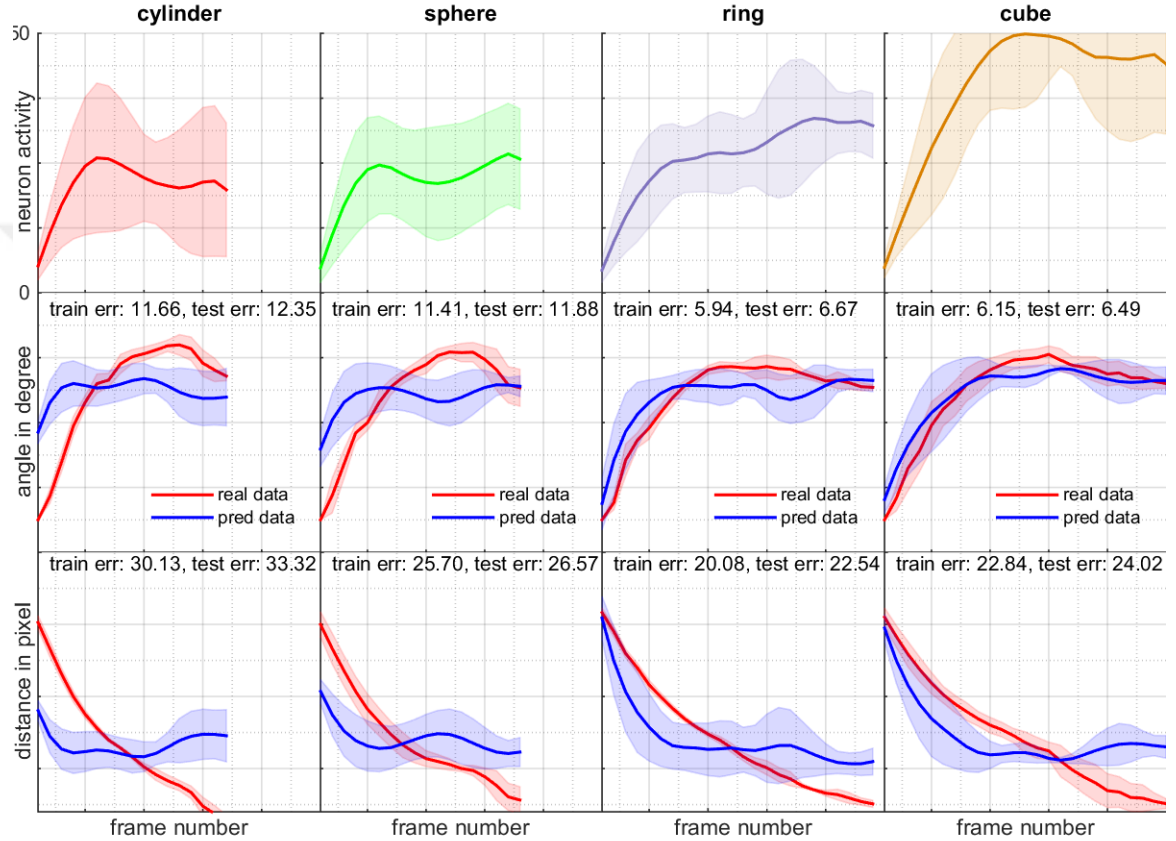


Figure 16: non-mirror neuron 449 performance as average \pm standard deviation over all the trials for each object: the first row is the average of the aggregated neural activity, second and third rows represent angle and distance respectively: blue curve is the average of extracted kinematics and the red curve is the average of the corresponding predicted kinematics.

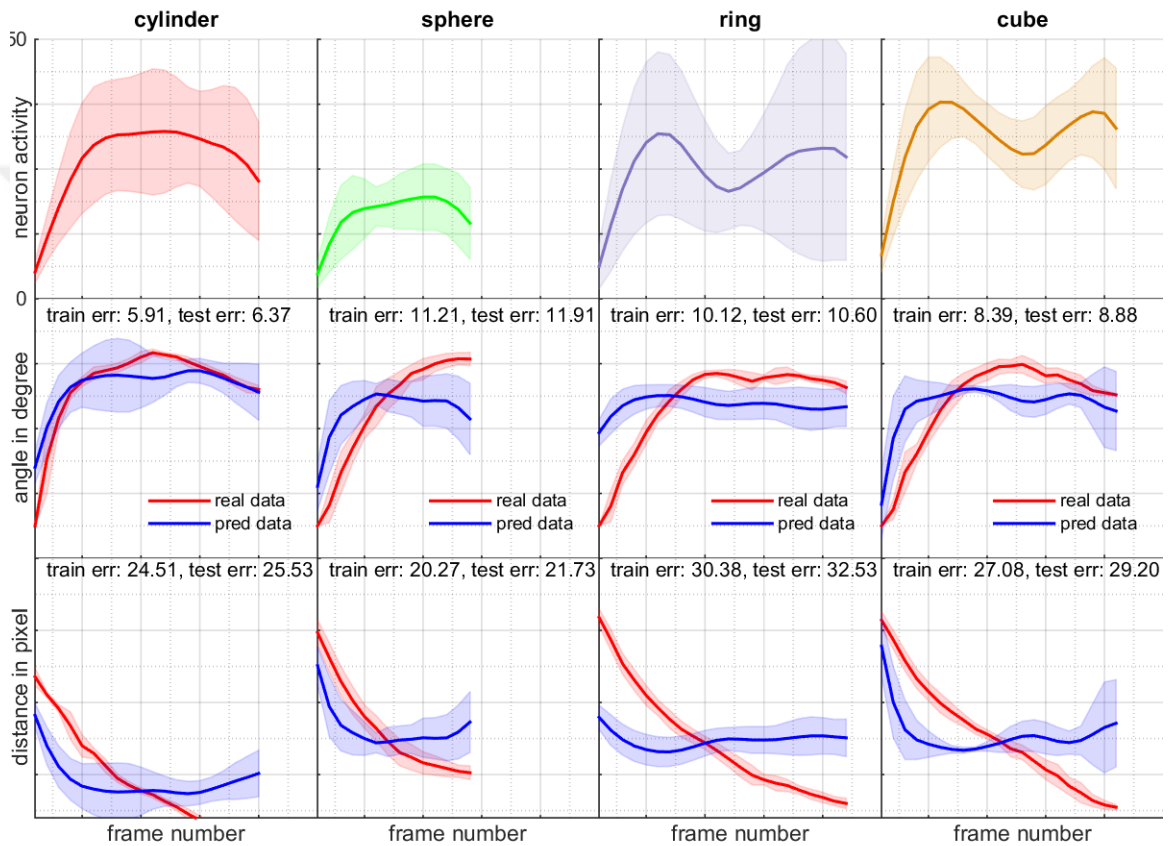


Figure 17: mirror neuron 453 performance as average \pm standard deviation over all the trials for each object: the first row is the average of the aggregated neural activity, second and third rows represent angle and distance respectively: blue curve is the average of extracted kinematics and the red curve is the average of the corresponding predicted kinematics.

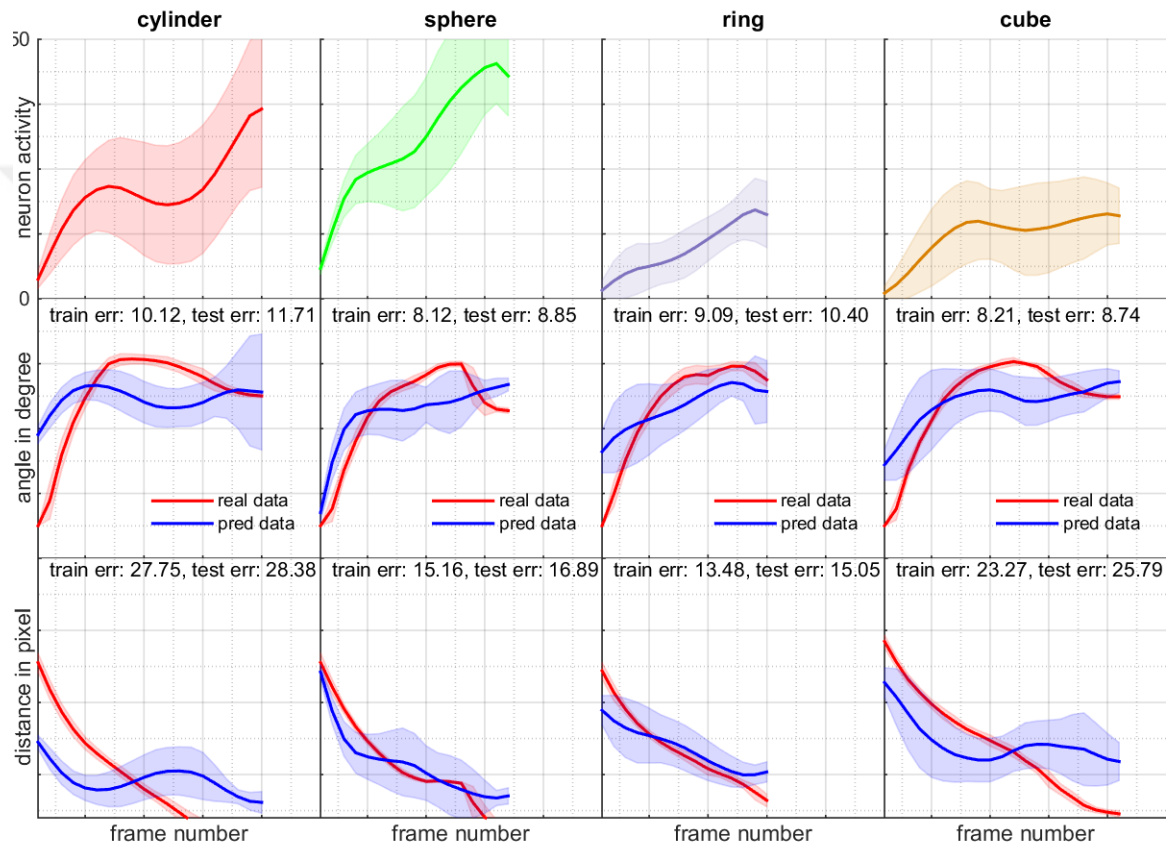


Figure 18: mirror neuron 479 performance as average \pm standard deviation over all the trials for each object: the first row is the average of the aggregated neural activity, second and third rows represent angle and distance respectively: blue curve is the average of extracted kinematics and the red curve is the average of the corresponding predicted kinematics.

APPENDIX B

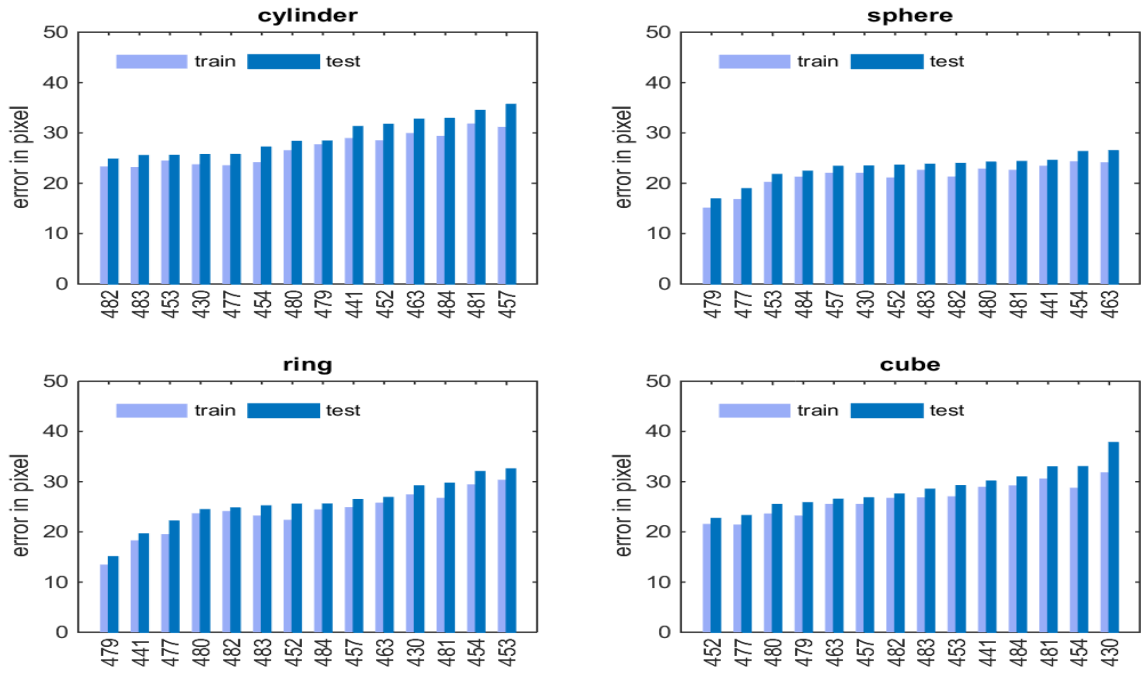


Figure 19: List of mirror neurons ordered based on their performance (test error) in decoding the distance data required for each object by using pre0-agg1 input, neurons number on horizontal axis

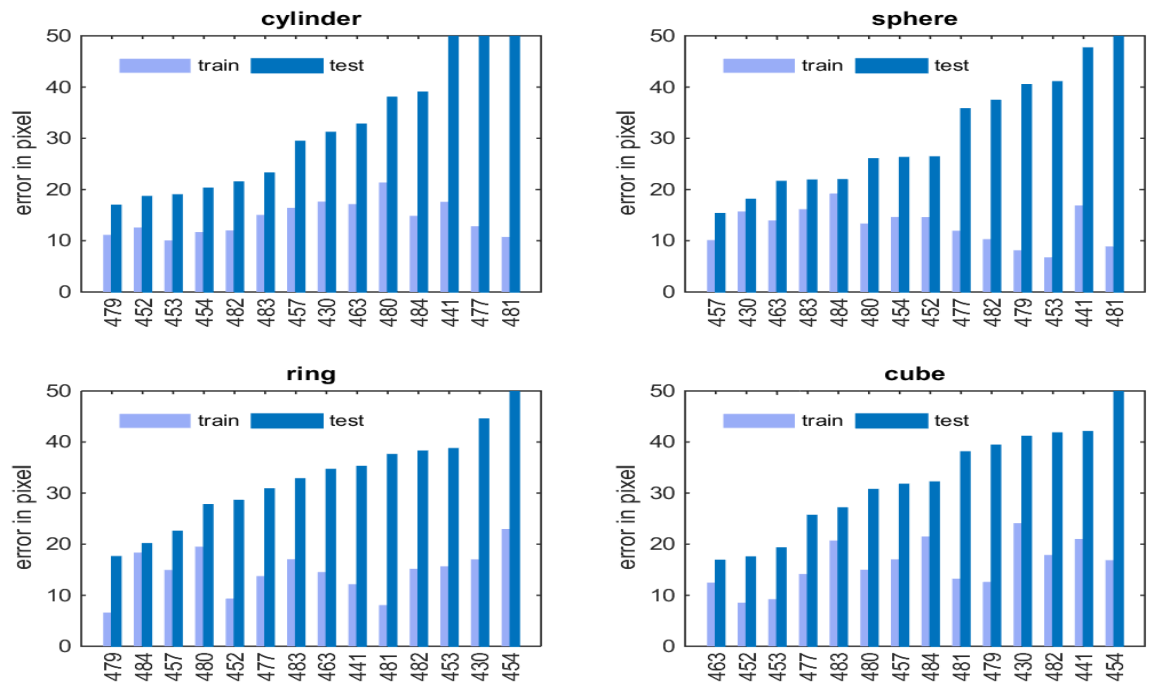


Figure 20: List of mirror neurons ordered based on their performance (test error) in decoding the distance data required for each object by using pre1-agg1 input, neurons number on horizontal axis

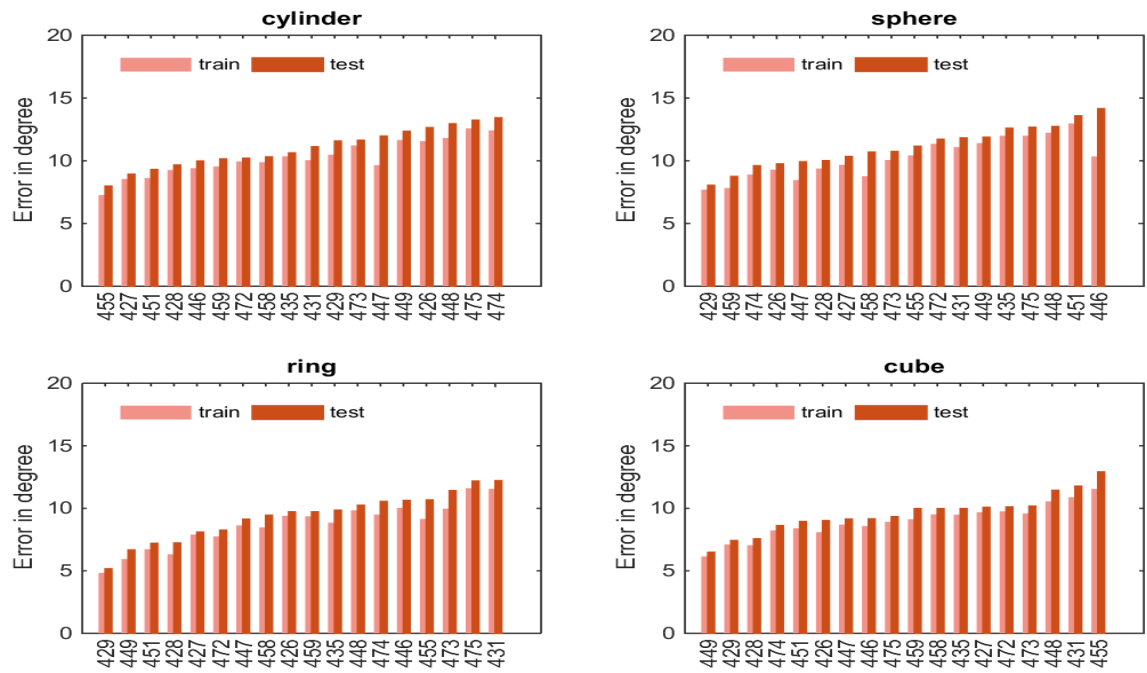


Figure 21: List of non-mirror neurons ordered based on their performance (test error) in decoding the angle data required for each object by using pre0-agg1 input, neurons number on horizontal axis

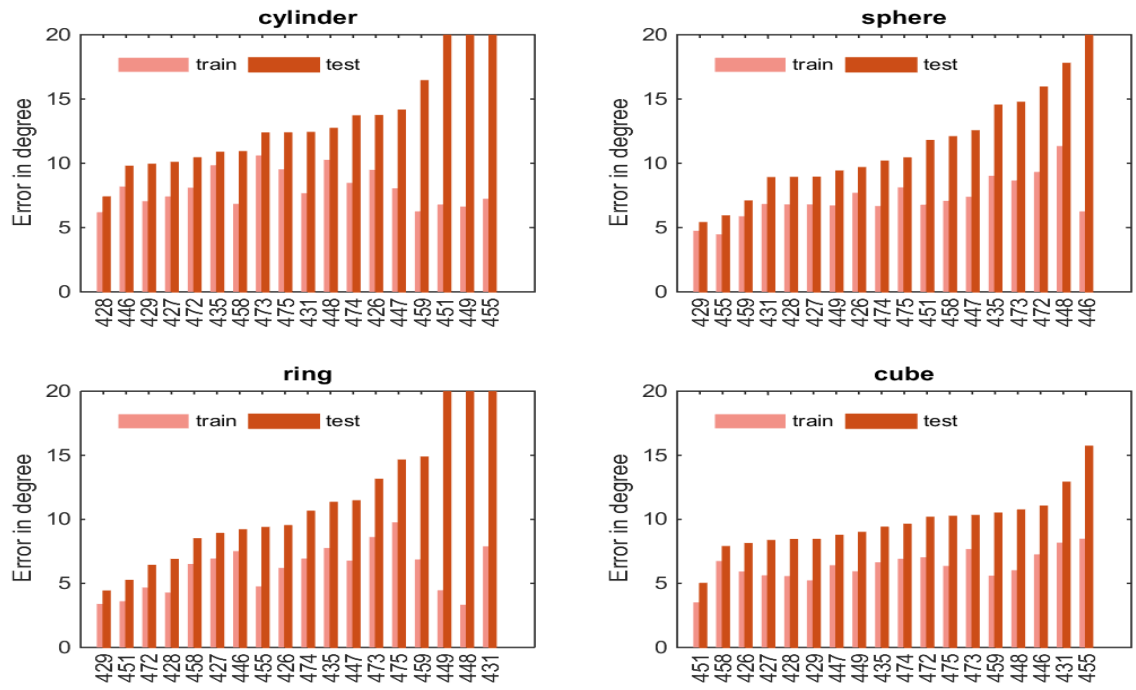


Figure 22: List of non-mirror neurons ordered based on their performance (test error) in decoding the angle data required for each object by using pre1-aggl input, neurons number on horizontal axis

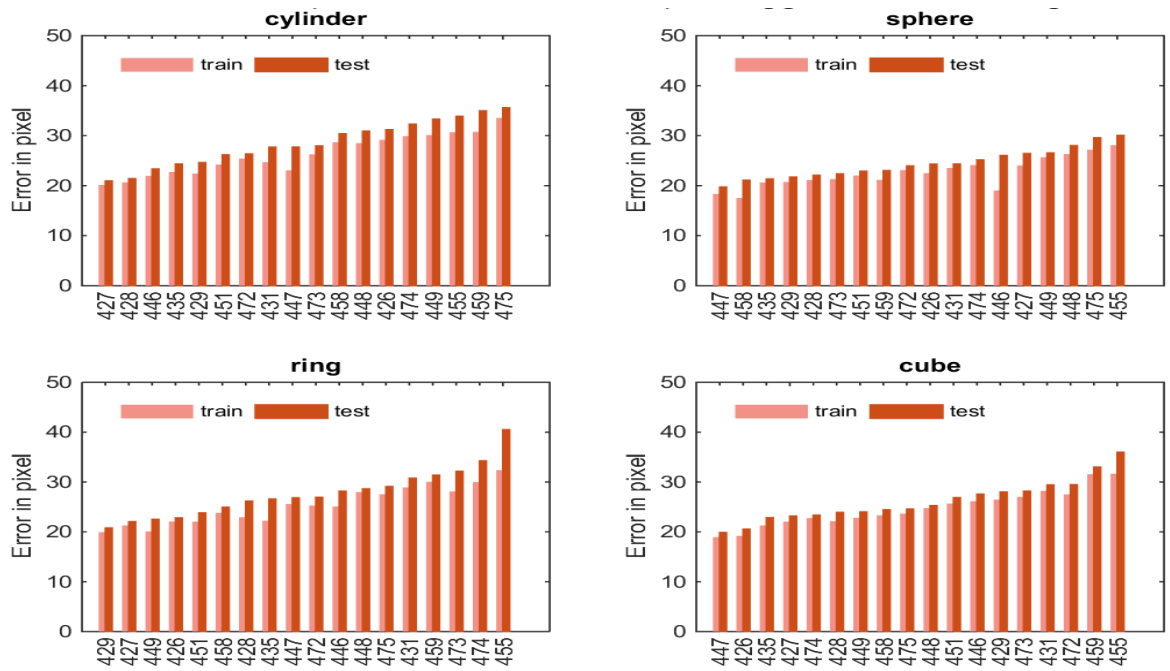


Figure 23: List of non-mirror neurons ordered based on their performance (test error) in decoding the angle data required for each object by using pre0-aggl input, neurons number on horizontal axis

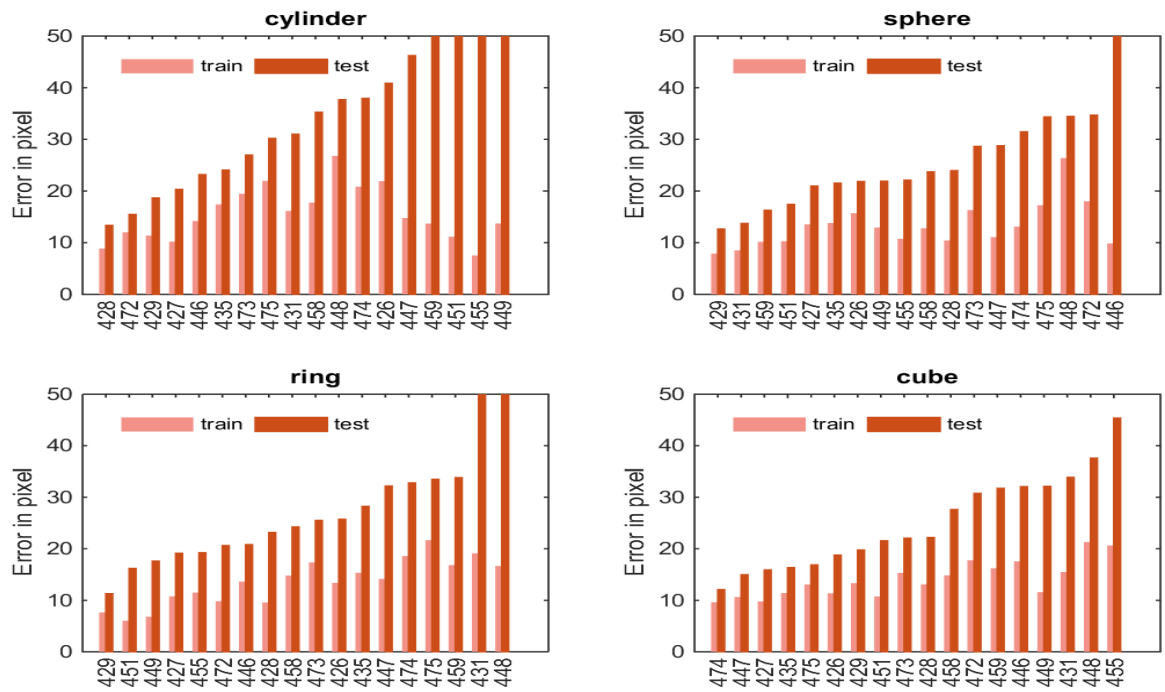


Figure 24: List of non-mirror neurons ordered based on their performance (test error) in decoding the distance data required for each object by using pre1-agg1 input, neurons number on horizontal axis

Bibliography

- [1] C. J. Bell, P. Shenoy, R. Chalodhorn, and R. P. Rao, “Control of a humanoid robot by a noninvasive brain–computer interface in humans,” *Journal of neural engineering*, vol. 5, no. 2, p. 214, 2008.
- [2] D. Floreano, A. J. Ijspeert, and S. Schaal, “Robotics and neuroscience,” *Current Biology*, vol. 24, no. 18, pp. R910–R920, 2014.
- [3] T. Trappenberg, *Fundamentals of computational neuroscience*. OUP Oxford, 2009.
- [4] S. Musallam, B. Corneil, B. Greger, H. Scherberger, and R. Andersen, “Cognitive control signals for neural prosthetics,” *Science*, vol. 305, no. 5681, pp. 258–262, 2004.
- [5] J. Carpaneto, V. Raos, M. A. Umiltà, L. Fogassi, A. Murata, V. Gallese, and S. Micera, “Continuous decoding of grasping tasks for a prospective implantable cortical neuroprosthesis,” *Journal of neuroengineering and rehabilitation*, vol. 9, no. 1, p. 84, 2012.
- [6] V. K. Menz, “Continuous detection and prediction of grasp states and kinematics from primate motor, premotor, and parietal cortex,” 2015.
- [7] K. D. Anderson, “Targeting recovery: priorities of the spinal cord-injured population,” *Journal of neurotrauma*, vol. 21, no. 10, pp. 1371–1383, 2004.
- [8] G. Rizzolatti, R. Camarda, L. Fogassi, M. Gentilucci, G. Luppino, and M. Matelli, “Functional organization of inferior area 6 in the macaque monkey,” *Experimental brain research*, vol. 71, no. 3, pp. 491–507, 1988.
- [9] G. Rizzolatti and L. Fadiga, “Grasping objects and grasping action meanings: the dual role of monkey rostroventral premotor cortex (area f5),” *Sensory guidance of movement*, vol. 218, pp. 81–103, 1998.
- [10] G. d. Pellegrino, L. Fadiga, L. Fogassi, V. Gallese, and G. Rizzolatti, “Understanding motor events: a neurophysiological study,” *Experimental brain research*, vol. 91, no. 1, pp. 176–180, 1992.
- [11] V. Gallese, L. Fadiga, L. Fogassi, and G. Rizzolatti, “Action recognition in the premotor cortex,” *Brain*, vol. 119, no. 2, pp. 593–609, 1996.
- [12] V. Gallese, L. Fadiga, L. Fogassi, and G. Rizzolatti, “Action recognition in the premotor cortex,” *Brain*, vol. 119, no. 2, pp. 593–609, 1996.
- [13] G. Rizzolatti, L. Fadiga, V. Gallese, and L. Fogassi, “Premotor cortex and the recognition of motor actions,” *Cognitive brain research*, vol. 3, no. 2, pp. 131–141, 1996.

- [14] G. Rizzolatti and L. Craighero, “Mirror neuron: a neurological approach to empathy,” *Neurobiology of human values*, pp. 107–123, 2005.
- [15] J. Carpaneto, V. Raos, M. A. Umiltà, L. Fogassi, A. Murata, V. Gallese, and S. Micera, “Continuous decoding of grasping tasks for a prospective implantable cortical neuroprosthesis,” *Journal of neuroengineering and rehabilitation*, vol. 9, no. 1, p. 84, 2012.
- [16] J. Carpaneto, M. Umiltà, L. Fogassi, A. Murata, V. Gallese, S. Micera, and V. Raos, “Decoding the activity of grasping neurons recorded from the ventral premotor area f5 of the macaque monkey,” *Neuroscience*, vol. 188, pp. 80–94, 2011.
- [17] Y. Hao, Q. Zhang, M. Controzzi, C. Cipriani, Y. Li, J. Li, S. Zhang, Y. Wang, W. Chen, M. C. Carrozza, *et al.*, “Distinct neural patterns enable grasp types decoding in monkey dorsal premotor cortex,” *Journal of neural engineering*, vol. 11, no. 6, p. 066011, 2014.
- [18] B. R. Townsend, E. Subasi, and H. Scherberger, “Grasp movement decoding from premotor and parietal cortex,” *Journal of Neuroscience*, vol. 31, no. 40, pp. 14386–14398, 2011.
- [19] Z. Xu, K. K. Ang, and C. Guan, “Neural decoding of movement targets by unsorted spike trains,” in *Acoustics, Speech and Signal Processing (ICASSP), 2013 IEEE International Conference on*, pp. 954–958, IEEE, 2013.
- [20] M. Maranesi, A. Livi, and L. Bonini, “Processing of own hand visual feedback during object grasping in ventral premotor mirror neurons,” *Journal of Neuroscience*, vol. 35, no. 34, pp. 11824–11829, 2015.
- [21] M. Kirtay, V. Papadourakis, V. Raos, and E. Oztop, “Neural representation in f5: cross-decoding from observation to execution,” *BMC Neuroscience*, vol. 16, no. Suppl 1, p. P190, 2015.
- [22] V. K. Menz, S. Schaffelhofer, and H. Scherberger, “Representation of continuous hand and arm movements in macaque areas m1, f5, and aip: a comparative decoding study,” *Journal of neural engineering*, vol. 12, no. 5, p. 056016, 2015.
- [23] V. Papadourakis and V. Raos, “Cue-dependent action-observation elicited responses in the ventral premotor cortex (area f5) of the macaque monkey,” in *Soc Neurosci Abstr*, p. 2, 2013.